# Deciphering the Complex Fluid History of a Greenstone-Hosted Gold Deposit: Fluid Inclusion and Stable Isotope Studies of the Giant Mine, Yellowknife, Northwest Territories, Canada

**Article** *in* Economic Geology · December 2004

DOI: 10.2113/gsecongeo.99.8.1643

CITATIONS
28

READS
136

**4 authors**, including:

Kevin Shelton
University of Missouri
**129** PUBLICATIONS **2,464** CITATIONS

SEE PROFILE

Edmond H.P. Van Hees
Oakland University
**37** PUBLICATIONS **278** CITATIONS

SEE PROFILE

Hendrik Falck
NWT Geological Survey
**166** PUBLICATIONS **1,041** CITATIONS

SEE PROFILE

©2004 by Economic Geology
Vol. 99, pp. 1643–1663

# Deciphering the Complex Fluid History of a Greenstone-Hosted Gold Deposit: Fluid Inclusion and Stable Isotope Studies of the Giant Mine, Yellowknife, Northwest Territories, Canada

Kevin L. Shelton,† Todd A. McMenamy,

*Department of Geological Sciences, University of Missouri, Columbia, Missouri 65211*

Edmond H. P. van Hees,

*Department of Geology, Wayne State University, Detroit, Michigan 48202*

and Hendrik Falck

*C. S. Lord Northern Geoscience Centre, P.O. Box 1320, Yellowknife, Northwest Territories, Canada X1A 2L9*

## Abstract

Mesothermal, greenstone-hosted gold deposits are typically products of complex hydrothermal systems that involved multiple fluids at various times throughout their histories. The Giant mine is an example of such an extremely complicated system, including (1) multiple, local and regional gold-depositing events; (2) at least two styles of gold ore introduction in the mine area, including both refractory, sulfide-hosted and free-milling, vein-hosted ores, whose relative timing is enigmatic; (3) fluid overprinting associated with deposition of multiple generations of postore vein- and vug-filling minerals; and (4) postore deformation and recrystallization of ore veins, especially along faults.

Three main stages of quartz-carbonate mineralization are recognized in the Giant mine. Stage I encompasses deposition of dominant refractory, sulfide-hosted ores and subordinate free-milling, vein-hosted gold ores. Refractory, metavolcanic rock-hosted orebodies are connected to metasedimentary rocks east of the mine by an east-dipping alteration zone characterized by a depletion in Na and enrichments in K, Ag, As, S, and Sb. Quartz veins within the wall-rock alteration zone have $\delta^{18}O$ values that decrease systematically from 14.7 per mil in deeper metasedimentary rocks toward 11.6 per mil in shallower metabasalts in the mine. This decrease is interpreted to indicate that $^{18}O$-enriched ore fluids originated in deeper, metasedimentary rocks and reacted extensively with wall rocks along the entire extent of their flow paths before depositing dominantly refractory gold ores within more $^{16}O$-enriched, shallower, Ti-rich tholeiitic metabasalts. Quartz ± carbonate veins related to these gold ores were deposited from $H_2O$-$CO_2$-NaCl fluids with $T_h$ values of 180° to 360°C and salinities of 4 to 9 wt percent NaCl equiv. Evidence of sporadic fluid unmixing indicates that gold was deposited at temperatures near 350°C and pressures of 1 to 2 kbars.

The $\delta^{18}O$ values (SMOW) of vein quartz (11.6–14.7‰) and calcite (8.6–14.1‰) within the ore-related wall-rock alteration zone indicate deposition from fluids ($\delta^{18}O_{water}$ = 4.4–9.8‰) that equilibrated with metasedimentary and metavolcanic rocks during greenschist metamorphism. The $\delta^{18}O$ values (8.6–11.4‰) of vein quartz that locally contains free gold, hosted in metavolcanic rocks outside of the ore-related alteration zone, indicate deposition from fluids with lower $\delta^{8}O_{water}$ values of 2.8 to 5.6 per mil. The difference in ranges of $\delta^{18}O_{water}$ values may indicate that multiple events were responsible for gold-bearing quartz veining, or alternatively, that fluids depositing veins within and outside of the alteration zone represented distinct fluid reservoirs that evolved through reaction with isotopically distinct rocks in their source regions (i.e., $^{18}O$-enriched metasedimentary vs. $^{16}O$-enriched metavolcanic rocks).

Postore (stage II) carbonate veins associated with minor Pb-Zn-Sb-Ag mineralization were deposited from highly saline NaCl-$CaCl_2$ brines with $T_m$ values of –32° to –36°C and $T_h$ values of 72° to 273°C. The $\delta^{18}O$ values of these carbonates (20.6–26.1‰) indicate that their parent brines ($\delta^{18}O_{water}$ = 9–14‰) also equilibrated with metasedimentary and metavolcanic rocks. Subsequent dissolution of these carbonate veins created abundant vuggy porosity.

Late (stage III), primarily vug-filling dolomite ± stibnite, overgrown by scalenohedral calcite, was deposited from dilute fluids (<6.0 wt % NaCl equiv) with $T_h$ values of 95° to 115°C. The $\delta^{18}O$ values of dolomite (17.4 toward 13.4‰) and latest calcite (10.9‰) indicate deposition from progressively less evolved meteoric waters with decreasing $\delta^{18}O$ values from 1.1 toward –6.9 per mil.

Refractory ores in the main alteration zone and gold-bearing quartz veins contained therein formed from chemically similar $CO_2$-$H_2O$-NaCl ore fluids whose oxygen isotope compositions are consistent with a metasedimentary source. These two styles of gold mineralization appear to be part of the same mineralizing event in which the style of mineralization was dictated by the mechanism of ore deposition. Refractory, sulfide-hosted gold mineralization resulted from reaction of mineralizing fluids with metavolcanic wall-rock $Fe^{2+}$. Free-milling, gold-bearing quartz vein ores were deposited as a result of fluid unmixing, with loss of $H_2S$ to the vapor phase.

† Corresponding author: e-mail, SheltonKL@missouri.edu

Gold-bearing quartz veins outside of the main wall-rock alteration zone in the Giant mine were also deposited by unmixing of similar $H_2O$-$CO_2$-NaCl fluids. However, these fluids were isotopically distinct from those within the alteration zone and may not be part of the refractory, sulfide-hosted gold-depositing event. They may instead represent a separate mineralizing event whose fluids and ore-forming constituents were derived solely from within metavolcanic rocks.

This overprinting of one event on the other may have been a necessary condition for the development of world-class gold deposits in the Yellowknife district. The important roles of both metavolcanic and metasedimentary source rocks may explain why some smaller greenstone belts, with limited volumes of metavolcanic rocks, can host substantial economic gold mineralization and has important implications for regional resource evaluation and exploration for gold deposits in greenstone belts.

## Introduction

Archean and Proterozoic greenstone-hosted gold deposits have produced a significant portion of the world's gold (Groves and Phillips, 1987; Woodall, 1988; Groves et al., 2003). Canadian Archean terranes have produced an estimated 8,000 t of gold, including 14 world-class gold deposits (i.e., >100 t Au; Robert and Poulsen, 1997). These deposits are products of complex hydrothermal systems involving multiple fluids at different times during their history as demonstrated by the presence of multiple generations of veins and various types of fluid inclusions. This makes it a challenge to look back through the numerous fluid overprints to deduce the chemistry of the gold ore fluid(s) and to determine the mechanism(s) of gold ore deposition.

The Giant gold mine, located in the 2.82 to 2.66 Ga (Isachsen and Bowring, 1994) Yellowknife greenstone belt, NWT, Canada (Figs. 1–2), is an example of such a system that is extremely complicated because of the presence of multiple, local and regional gold-depositing events (Falck, 1992; Kerswill et al., 2002), at least two styles of gold ore introduction in the mine area, including both refractory sulfide- and vein-hosted ores, fluid overprinting associated with deposition of multiple generations of postore vein- and vug-filling minerals, and postore deformation and recrystallization of ore veins, especially along faults. The disseminated nature of gold ore and the scarcity of ore-related fluid inclusions contribute to the difficulty of studying the hydrothermal fluid evolution of the Giant mine.

### *Multiple fluids in mesothermal gold deposits*

Studies of greenstone-hosted mesothermal gold deposits have documented that ore fluids typically are low-salinity (< ~6–10 wt % NaCl equiv), aqueous-carbonic fluids, with low to moderate $CO_2$ contents (5–20 mol %; Robert and Kelly, 1987; Kerrich and Fyfe, 1988; Kerrich and Kamineni, 1988; Kesler, 1991; Ho et al., 1992; Samson et al., 1997). The composition of the ore fluid is indicated by abundant $H_2O$-$CO_2$- and $CO_2$-rich fluid inclusions found in gold-bearing quartz veins and by textural evidence showing gold crystals and these fluid inclusions in the same healed fractures (Robert and Kelly, 1987). Many investigations have also revealed the presence of aqueous fluid inclusions in mesothermal gold systems. These aqueous inclusions have been variously interpreted to represent (1) fluids integral to the ore-forming event (Nesbitt et al., 1986), (2) postore fluids (So et al., 1995; Jia et al., 2003), or (3) synore fluids that are not the ore fluid (Goldfarb et al., 1988).

Based on $\delta$D values of inclusion fluids, Nesbitt et al. (1986) interpreted Jurassic to Tertiary orogenic mesothermal gold

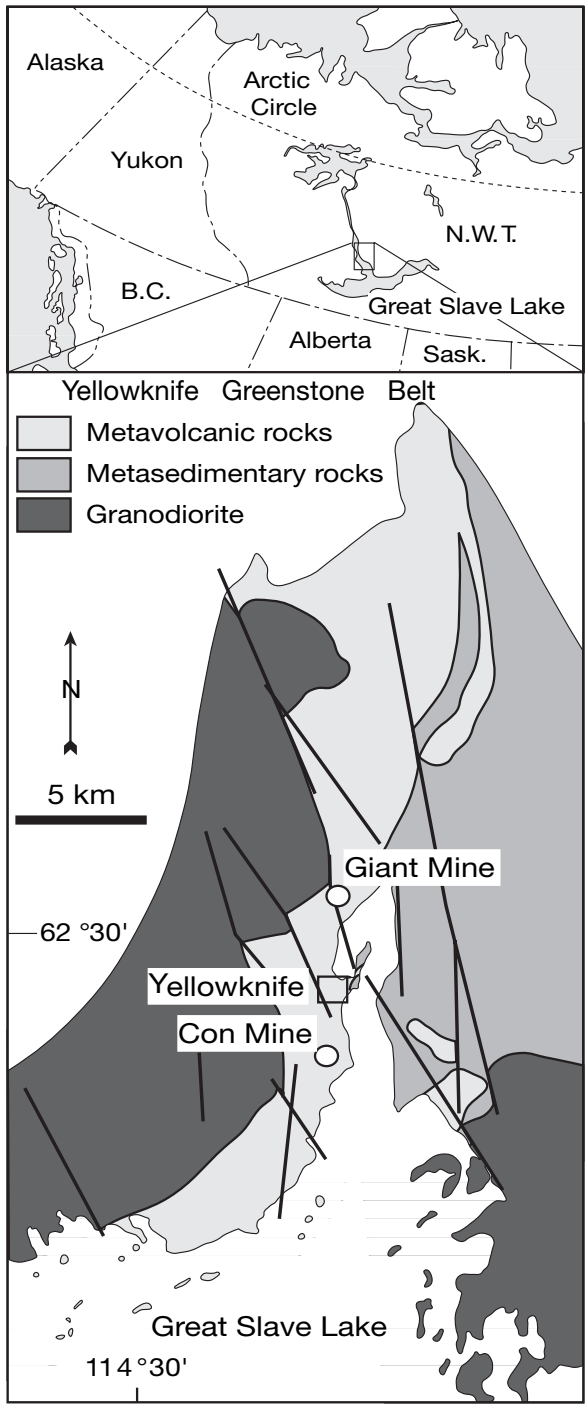


Fig. 1. Location map of the Giant mine within the Yellowknife greenstone belt, NWT, Canada. Black lines indicate faults.

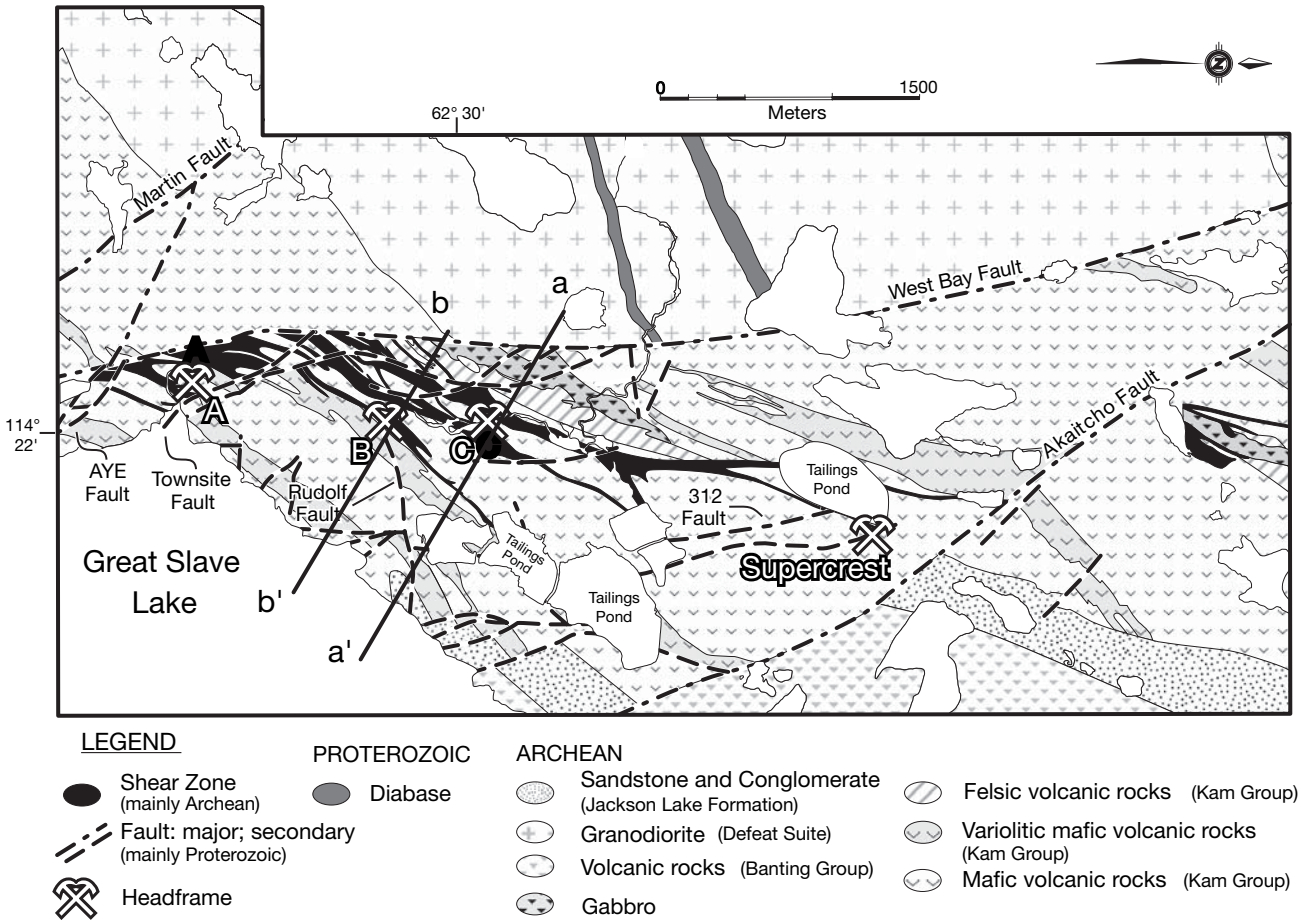


FIG. 2. Geologic map of the Giant mine area, showing locations of major orebodies (headframes) and faults. Latitude and longitude are for the C ore shaft. Lines labeled a-a' and b-b' indicate locations of cross sections in Figures 3 and 4.

deposits of the Canadian Cordillera to be derived from evolved meteoric waters. Nesbitt et al. (1986) extended the meteoric model to Archean lode gold deposits, based on the similarities in geology and geochemistry among Archean and Cordilleran mesothermal gold deposits. Shelton et al. (1988) showed that highly evolved meteoric waters were involved in the formation of Jurassic, intrusion-related mesothermal gold deposits in Korea, potentially validating a more general application of meteoric models to the formation of mesothermal gold deposits.

Pickthorn et al. (1987a, b) and Goldfarb et al. (1988) rejected the application of the meteoric model to other mesothermal gold deposits. They favored connate waters or fluids generated during prograde metamorphic reactions as the main component of ore fluids in mesothermal deposits and viewed the aqueous inclusions as later fluids, genetically unrelated to ore formation. Using N, H, and O isotopes, Jia et al. (2003) demonstrated a likely deep crustal source for ore-forming fluids in orogenic gold-bearing quartz vein deposits in North America, most likely of metamorphic origin.

Some of the enigmatic aqueous inclusions in Precambrian greenstone-hosted gold deposits have such high salinities (>10 wt % NaCl equiv) and/or low homogenization temperatures (<250°C) that they require a special explanation (Walsh et al., 1988; de Ronde et al., 1992). These inclusions have been interpreted as primary products of phase separation from $H_2O$-$CO_2$-NaCl ore fluids (Robert and Kelly, 1987; Samson et al., 1997) because of the preferential fractionation of almost all the salt into the $H_2O$-rich phase during unmixing (Bowers and Helgeson, 1983). They have also been interpreted as secondary inclusions unrelated to ore, formed from basement brines (Burrows and Spooner, 1990; Kerrich and King, 1993; Fayek and Kyser, 1995; Boullier et al., 1998).

In this paper we address the origin of $CO_2$-rich, $H_2O$-$CO_2$, and aqueous fluid inclusions found in the Giant gold mine ore system. By combining stable isotope and fluid inclusion techniques we are able to see through the complexity of various fluid overprints and to suggest likely ore fluid sources and ore-depositing mechanisms.

## Regional Geology

The Giant mine, Canada's seventh largest gold producer (~250 metric tons (t) of gold), is located in the Yellowknife greenstone belt on the southwestern margin of the Slave structural province (Figs. 1–2). Metavolcanic rocks of the Yellowknife mining district have been separated into three units, from oldest to youngest, the Central Slave Cover (Dwyer Lake Formation, 2853–2821 Ma; Isachsen, 1992; Bleeker et al., 1999; Ketchum and Bleeker, 2000), the Kam Group (2.72–2.70 Ga; Isachsen and Bowring, 1997), and the Banting

Group (2664–2662 Ma; Isachsen and Bowring, 1997), with the Kam Group comprising most of the greenstone belt (Helmstaedt and Padgham, 1986a, b). These three major stratigraphic units represent discrete periods of mafic to felsic volcanism. To the east of the greenstone belt, conformably overlying the Banting Group, is a thick sequence of volcanic-derived metasedimentary rocks, known as the Duncan Lake Group (Henderson, 1970, 1975), deposited around 2661 ± 2 Ma (Bleeker and Villeneuve 1995).

The Western Granodiorite, a multiphase, granodioritic complex of the Defeat Suite (Figs. 1–3a), intruded the metavolcanic rocks from the west between 2634 and 2605 Ma (Atkinson and van Breeman, 1990; MacLachlan and Davis, 2002). Shear zone formation is thought to be associated with lateral shortening and tilting of the volcanic sequence and intrusion of the granodiorite (Brown et al., 1959; Boyle, 1961; Henderson and Brown, 1966; Helmstaedt and Padgham, 1986a). The metamorphic grade of country rocks, related to regional metamorphism and synchronous emplacement of the Western Granodiorite, is amphibolite facies at the granitic batholith-metavolcanic rock contact on the west side of the mine. These rocks are in fault contact with greenschist facies metavolcanic and metasedimentary rocks on the east (Drury, 1977; Thompson, 2002). Two other granitic masses occur in the district, the Prosperous Lake granite (2596 ± 2 Ma, Davis and Bleeker, 1999) to the north of the metasedimentary rocks and the Southeastern Granodiorite Complex (2644 ± 5 Ma, Davis and Bleeker, 1999) to the south (Henderson, 1985).

The Yellowknife greenstone belt and associated ore deposits have been cut by a system of north-northwest–trending Proterozoic strike-slip faults (the West Bay, Kam-Pud, and Hay-Duck faults) that are connected by smaller cross-over faults (Akaitcho, Martin, AYE, and Townsite faults, Fig. 2; Helmstaedt and Bailey, 1987). Horizontal and vertical offsets along the West Bay fault are ~4,900 and ~500 m, respectively (Campbell, 1947; Brown, 1955).

### *Gold mineralization*

Regionally, two principal styles of gold mineralization are recognized in the Yellowknife district (Falck, 1992; Kerswill and Falck, 2002; Kerswill et al., 2002): a refractory style that characterizes much of the carbonate-rich ore with fine-grained pyrite, arsenopyrite, and sulfosalts hosted by early veins and sericite schist alteration zones in the Giant-Con mine system; and a free-milling style that is developed at the regional scale. The free-milling style includes (1) gold with sphalerite, galena, and chalcopyrite in the later veins of the Con-Giant mine system; (2) gold in veins with megacrystic sulfides, including pyrite and arsenopyrite; (3) gold with sphalerite and galena in arsenopyrite-poor veins; (4) gold in pyrite- and chalcopyrite-rich veins; and (e) molybdenite-bearing auriferous veins. Superposition of different styles at numerous locales enhances the total metal endowment, but later deformation and overprinting have blurred temporal relationships.

### *Giant mine*

Disseminated, refractory (sulfide-hosted) and lesser free milling, vein-hosted mineralization in the Giant mine extends for 6.5 km along strike in the pillowed, pillow-breccia, and massive basalts of the Kam Group (Fig. 2). Mineralization differs from typical mesothermal deposits in that it has a limited depth extent (~600 m, Figs. 3a, 4a) and anomalously high As and Sb concentrations reflected in abundant arsenopyrite and stibnite (van Hees et al., 1999; van Hees and Shelton,

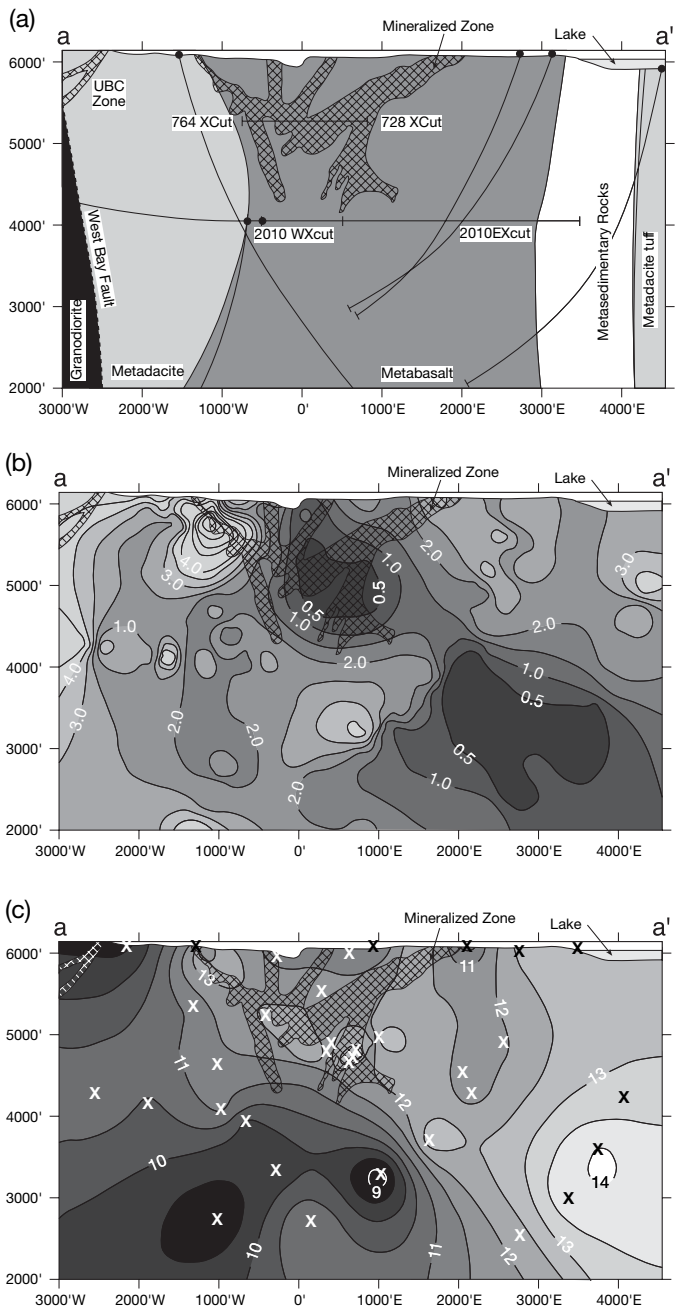


FIG. 3. Cross sections across the Giant mine (a-a' in Fig. 2) showing (a) geology as well as deep drill holes and underground crosscuts (Xcut, shown by thin black lines), (b) contoured values of $Na_2O$ (wt %) in whole-rock samples, and (c) contoured values of $\delta^{18}O$ values of quartz (from van Hees et al., 1999). X = sample localities used in defining isotope contours. Contour interval is 0.5 per mil. Scale is in feet consistent with the mine grid. Darker shaded areas in (b) coincide with wall-rock alteration zone that corresponds to enrichments in $K_2O$, Ag, Sb, As, S, $^{18}O$ and depletion in $Na_2O$ (van Hees et al., 1999). Outlined hatched areas are known ore zones comprising the mineralized zone.

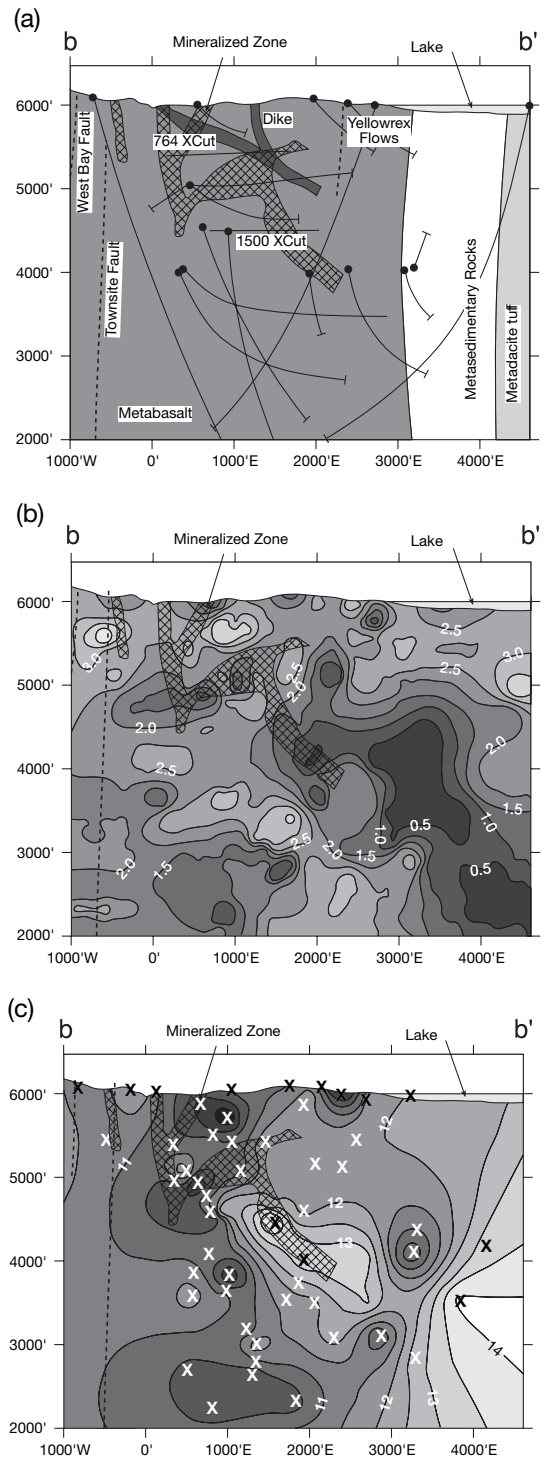


FIG. 4. Cross sections across the Giant mine (b-b' in Fig. 2) showing (a) geology as well as deep drill holes and underground crosscuts (Xcut, shown by thin black lines), (b) contoured values of $Na_2O$ (wt %) in whole-rock samples (van Hees et al., 2004), and (c) contoured values of $\delta^{18}O$ values of quartz (this study). X = sample localities used in defining isotope contours. Contour interval is 0.5 per mil. Scale is in feet consistent with the mine grid. Darker shaded areas in (b) coincide with wall-rock alteration zone that corresponds to enrichments in $K_2O$, Ag, Sb, As, S, $^{18}O$, and depletion in $Na_2O$ (van Hees et al., 1999). Outlined hatched areas are known ore zones comprising the mineralized zone.

2002b). Wall-rock–hosted ore and quartz-carbonate veining are enveloped by sericite-carbonate alteration grading to chlorite-carbonate schist. Except for the occurrence of free gold in some of the subordinate quartz-carbonate veins, the Giant orebodies are dominated by refractory ore, with gold most commonly occurring in arsenopyrite and to a lesser extent in pyrite (Coleman, 1957; Boyle, 1961; Brown, 1992; Steffanski and Halverson, 1992).

The strongly sericitized and deformed ore-hosting metavolcanic rocks are considered part of the Giant-Campbell shear zone. Early studies concluded that shear zones were the dominant control on gold deposition (Campbell, 1947; Dadson and Bateman, 1948; Lord, 1951; Coleman, 1957; Boyle, 1961; Henderson and Brown, 1966; Kerrich and Allison, 1978; Kerrich, 1981). However, mapping of the Giant orebodies by Brown and Dadson (1953), Brown et al. (1959), and Barclay (1996 unpub. company rept.) revealed features more consistent with the deposit being hosted by a folded lithologic unit rather than a shear zone. Brown (1992) questioned the role of the Giant-Campbell shear zone in the formation of the Giant deposit, because most deformation of the host rocks postdates emplacement of the gold ore. Helmstaedt and Padgham (1986a, b) also questioned shear zone control on gold deposition. They pointed out that, although shear zones occur throughout the greenstone belt, ore-producing zones are concentrated in the Yellowknife Bay Formation, the uppermost member of the Kam Group.

Lithogeochemical studies by van Hees et al. (1999) revealed that the Giant deposits might lie preferentially within high Ti metabasalts. Van Hees et al. (1999, 2004) also found that the metavolcanic, wall-rock–hosted, refractory orebodies are connected to metasedimentary rocks east of the mine by an east-dipping alteration zone characterized by a depletion in Na (Figs. 3b, 4b) and enrichments in K, Ag, As, S, and Sb. Reactions between ore fluids and high Ti metavolcanic host rocks resulted in precipitation of wall-rock–hosted, refractory gold mineralization. The Yellowknife River fault zone, an Archean fault that separates the Kam Group from the Banting Group, may have provided a conduit for ore fluids and the extensive metasedimentary rock sequence to the east provided a source of fluids, metals, and ore-forming constituents (Falck et al., 1999; van Hees et al., 1999, 2004).

From a geochemical standpoint, the refractory ore of the Giant mine is a metasedimentary-type gold deposit hosted in metavolcanic rocks (van Hees et al., 1999). The short vertical extent (~600 m) of the ore zone, compared to typical shear zone-related mesothermal deposits (>2,000 m), is interpreted to reflect the near-horizontal intersection of the ore fluid conduit with ore-hosting high Ti metabasalts (van Hees et al., 1999). A fluid source in the metasedimentary rocks also explains the anomalously high Sb and As contents of the Giant ores (Robert, 1990). van Hees et al. (1999) could not determine unequivocally the source of gold in the Giant mine. However, metasedimentary rocks in the Yellowknife district, which were derived primarily from mafic volcanic rocks (Henderson, 1972), were considered to be a possible source for gold.

Whereas the refractory-disseminated ores of the Giant mine are restricted to mafic metavolcanic rocks, subordinate high-grade gold-bearing quartz veins occur both within and

outside of zones of wall-rock–hosted ore enveloped by sericite-carbonate alteration and are found in all lithologies preserved in the Yellowknife area, with the exception of Proterozoic dikes (Falck, 1992). High-grade, gold-bearing quartz veins may represent distinct ore fluids and ore events or they may, in part, be the result of the same ore fluid system that deposited refractory gold ores.

*Age of gold deposition*

The absolute timing of gold ore mineralization in the Yellowknife district remains enigmatic at both the deposit and regional scales (see Kerswill et al., 2002). Ootes et al. (2002), based on U-Pb dating of intrusions and Re-Os dating of molybdenite, suggested that an early phase of Mo (±Au) mineralization in the Yellowknife district was coincident with Banting age intrusions (Fig. 2, ~2.67 Ga).

The relative timing of free-milling and refractory ores in the Giant and Con mines is not fully understood and is complicated by the possibility that there are multiple gold-bearing quartz vein-forming events. Armstrong (1997) noted that deposition of some free-milling gold ore may have predated refractory ore at the Con mine. Based on structural evidence, Siddorn and Cruden (2000) suggested that most free-milling gold-bearing quartz veins at the Giant mine postdate wall-rock–hosted refractory gold ores. Refractory gold ores were thought to be synchronous with development of $S_1$ foliation during $D_1$ deformation (pre 2.64–2.62 Ga). Free-milling gold-bearing quartz veins may be associated with $D_2$ deformation (post-2.62 Ga, syn-2.58 Ga), an event that started during cooling of the Western Granodiorite and that modified and reactivated $D_1$ brittle-ductile fault zones (Siddorn and Cruden, 2000; Siddorn et al., 2005).

## Quartz and Carbonate Vein Paragenesis

At least three stages of quartz-carbonate mineralization have been recognized in the Giant mine: I, an early, gold-related, quartz-carbonate-sulfide stage; II, a postgold ore, carbonate stage; and III, a late, primarily vug-filling, carbonate stage (Fig. 5).

*Stage I*

Stage I includes economic quantities of gold and corresponds to the oldest quartz-carbonate-sulfide vein set described by Boyle (1954, 1961). The ore consists of broad zones of refractory, wall-rock–hosted mineralization with subordinate free-milling, quartz-carbonate veins (Fig. 6a-c). The relative timing of free-milling and refractory ores is unclear and is complicated by the possibility that there were multiple gold-bearing quartz vein-forming events during stage I.

Extensive alteration of wall rocks occurred during this initial period of mineralization. In general, disseminated mineralization and quartz-carbonate veining are enveloped by a brown-colored, sericite-carbonate-sulfide alteration that grades into green-colored, chlorite-carbonate schist. Gold in the wall rocks occurs dominantly as refractory ore, associated commonly with arsenopyrite and pyrite (Coleman, 1957; Boyle, 1961; Brown, 1992). In some of the subordinate quartz-carbonate veins in the north and central parts of the mine, gold occurs as free gold (Brown, 1992).

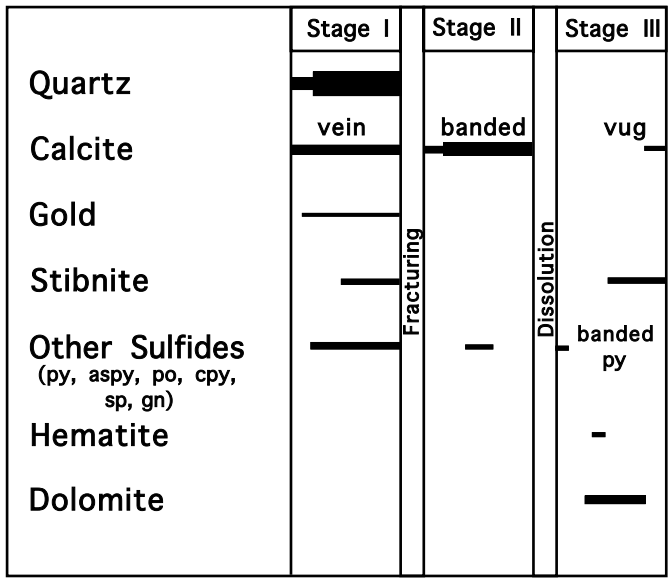


FIG. 5. Generalized paragenetic sequence of hydrothermal vein and vug-filling minerals from the Giant mine. Abbreviations: aspy = arsenopyrite, cpy = chalcopyrite, gn = galena, py = pyrite, po = pyrrhotite, sp = sphalerite.

Stage I veins are characterized by medium-grained (0.3–1.0 mm), milky-white quartz with lesser amounts of carbonates and sulfides (Fig. 6b-c). This quartz is often bordered and cut by later, clear, microcrystalline (<0.2 mm) quartz that typically contains no fluid inclusions. The amount of microcrystalline quartz varies from approximately 20 to 80 percent of the quartz in any given thin section, a limiting factor in performing fluid inclusions studies. Boyle (1954) attributed the origin of this microcrystalline quartz to crushing and recrystallization of the early, medium-grained quartz.

Carbonate in early gold-bearing quartz veins and in alteration zones is dominantly calcite and ankerite. In veins, it occurs as irregular masses and euhedral, rhombic crystals enclosed in quartz.

The principal sulfides introduced during stage I are pyrite, arsenopyrite, and locally pyrrhotite, chalcopyrite, sphalerite, stibnite, galena, and sulfosalts. Pyrite and arsenopyrite occur as disseminated euhedral to subhedral grains and bands in quartz veins or as fine disseminated crystals in cherty silica-rich schist. Pyrite and arsenopyrite grains are commonly fractured, consistent with the orebodies having experienced a later episode of deformation (Coleman, 1957).

*Stage II*

Stage II mineralization consists of fracture-filling calcite and stringers as well as lenses of banded carbonates with minor sulfides, dominantly pyrite, galena, sphalerite, and stibnite. Stage II fractures cut stage I quartz-carbonate veins (Fig. 6d) and are filled commonly by white to pink, finely crystalline calcite. Stage II stringers and lenses display early bands of white, tan, yellow, and pink, finely crystalline calcite (Fig. 7). The banded calcite commonly contains an inner zone of later, vug-filling red-brown to black calcite. In these samples, a dissolution surface cuts across the banded calcite, creating secondary vuggy porosity prior to stage III mineralization. A

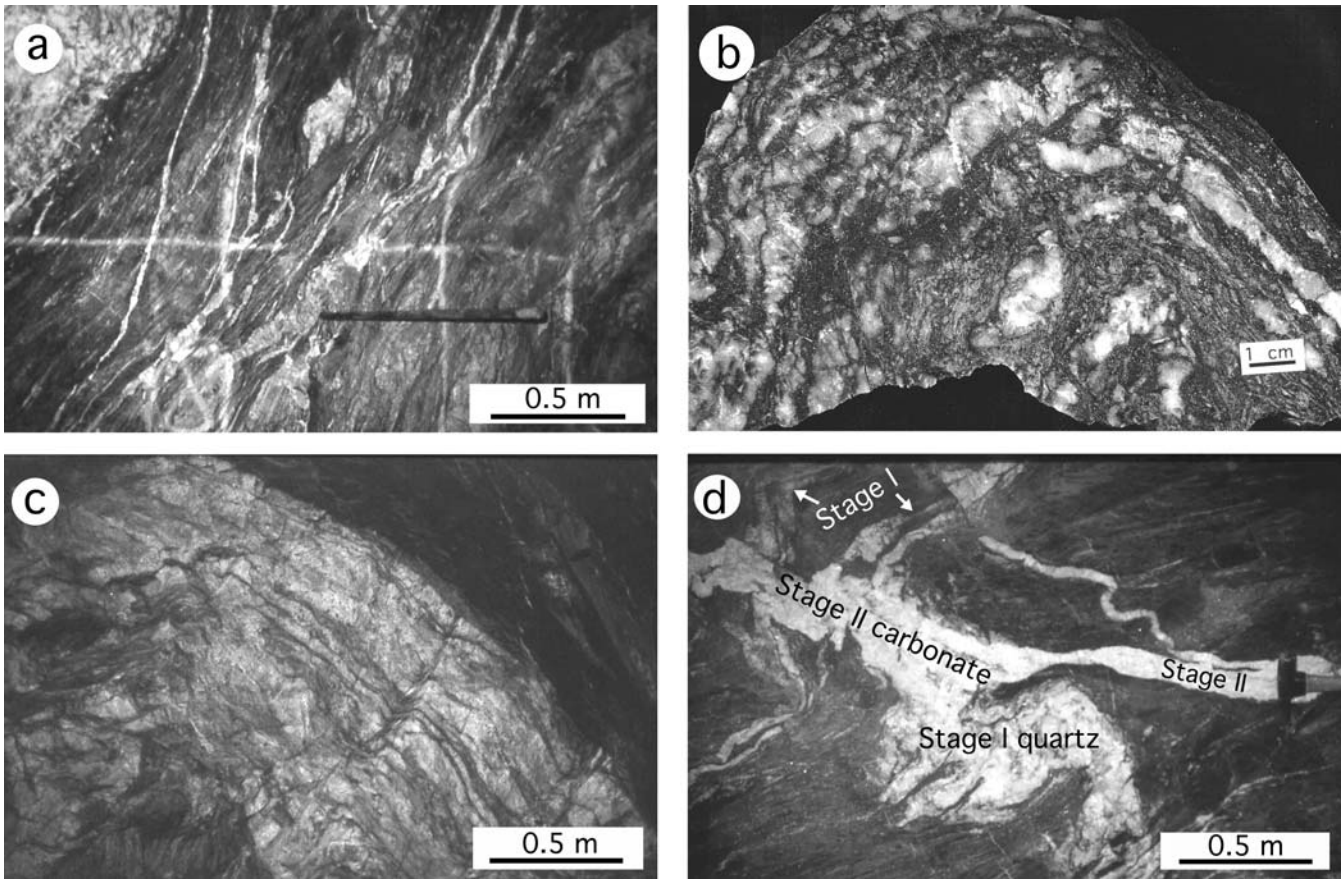


FIG. 6. Ore mineralization in the Giant mine. (a). Stage I refractory, sulfide-hosted gold ore in altered wall rock adjacent to large quartz vein in upper left corner. Note drill rod and painted drilling grid. (b). Stage I ore sample (75,600 ppb Au) from the Supercrest area of the Giant mine, demonstrating the deformed nature of the ore. The white areas are folded quartz veins in a tan matrix of sericitized mafic volcanic wall rock. Sulfide minerals are present as coarse pyrite cubes and fine gray fracture fillings associated with gold (dominantly arsenopyrite and Pb-Sb-Bi sulfosalts). Photograph courtesy of J. Kerswill, Geological Survey of Canada, Ottawa. (c). Stage I native gold-bearing, ribboned quartz vein. (d). Stage II carbonate vein crosscutting deformed stage I quartz veins.

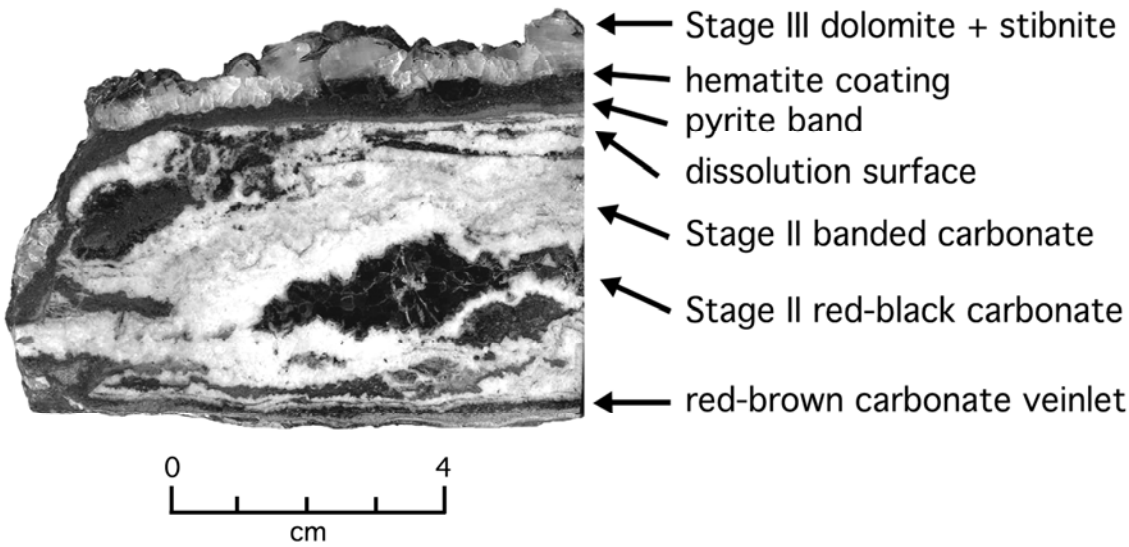


FIG. 7. Stage II banded carbonate vein sample KS96-14, showing banded pyrite, dissolution surface and stage III vug-filling dolomite.

thin band (<1.0 mm) of finely crystalline pyrite was precipitated on the dissolution surfaces and was later partially oxidized, forming a thin coat of hematite. Assays of stage II calcite veins show up to 70 ppm silver and 8 ppm gold.

*Stage III*

Stage III mineralization began with the growth of tan to clear, vug-filling, curved, rhombohedra of dolomite (up to 2.0 cm long) overgrowing stage II banded carbonates (Fig. 7). Large (<10 cm long) sprays of bladed stibnite are intergrown locally with dolomite and project into vugs. Late, clear to gray scalenohedral calcite crystals overgrow stage III dolomite.

## Fluid Inclusion Studies

Fifty samples of quartz and calcite from underground ore stopes and surface exposures were prepared as 100-$\mu$m-thick, doubly polished sections for fluid inclusion study. The variability in the abundance and quality of fluid inclusions resulted in 11 of the doubly polished plates not yielding any fluid inclusion data and 12 providing only a limited number of fluid inclusions. The quartz samples that lack fluid inclusions are located adjacent to the West Bay fault (Fig. 2) and Western Granodiorite and contain a large percentage of clear, microcrystalline quartz or are from silica-rich schist. Microthermometric data were obtained using a FLUID Inc. gas-flow heating/freezing stage calibrated with pure $CO_2$ and $H_2O$ inclusions (Shelton and Orville, 1980). Temperatures of total homogenization ($T_h$) have standard errors of ±2°C, and temperatures of melting ($T_m$ of ice, clathrate, and $CO_2$) and homogenization of $CO_2$-rich phases have standard errors of ±0.2°C. The composition and density of the trapped fluids were determined from thermometric data using the MacFlinCor software (Brown and Hagemann, 1995) and the compiled data of Kerrick and Jacobs (1981), Bodnar and Vityk (1994), and Thiery et al. (1994).

*Occurrence and compositional types of fluid inclusions*

Fluid inclusions were found in stage I massive quartz and carbonate veins, in quartz grains from silicified wall rock, and in stage II and III vug-filling calcite and dolomite. The size of fluid inclusions ranges from <1 to 25 $\mu$m with most inclusions <5 $\mu$m in size.

Three compositional types of fluid inclusions have been identified on the basis of their phase relationships at 20°C, combined with their behavior during cooling and slight heating. In order of decreasing abundance, they are carbonic ($CO_2$ ± $CH_4$) inclusions, aqueous inclusions, and $H_2O$-$CO_2$ inclusions (Fig. 8).

*Carbonic inclusions:* These fluid inclusions are composed dominantly of a $CO_2$-rich ($CO_2$ ± $CH_4$) liquid phase that upon

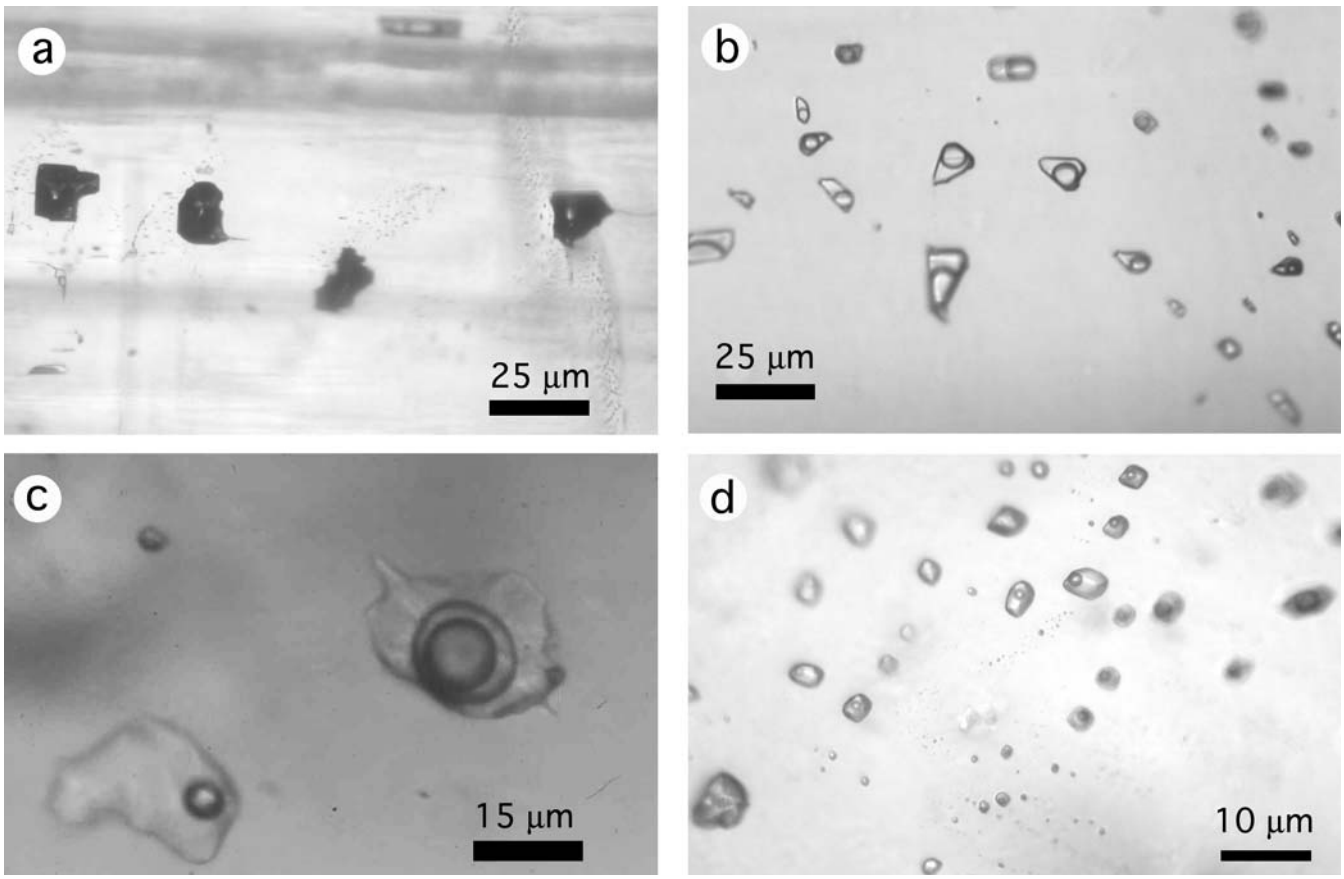


FIG. 8. Photomicrographs showing fluid inclusion types in stage I quartz of the Giant mine. (a). Problematic dark carbonic fluid inclusions at –25°C. (b). Two-phase, $H_2O$-$CO_2$ inclusions at 20°C. (c). Primary three-phase, $H_2O$-$CO_2$ inclusion with two-phase, water-rich $H_2O$-$CO_2$ inclusion at 3°C. (d). Secondary, two-phase, water-rich inclusions at 20°C.

cooling to <–20°C developed a $CO_2$-rich vapor bubble (Fig. 8a). These inclusions rarely have a thin rim of liquid water along the inclusion walls comprising <5 vol percent of the inclusion volume. Carbonic inclusions are found exclusively in early stage I quartz-carbonate veins and in quartz grains from silicified wall rock. They occur largely in medium-sized quartz grains as dark, hexagonal to irregularly shaped inclusions that are distributed randomly or occur along planes that mark growth zones, indicating that they are primary to pseudosecondary in origin (cf. Roedder, 1984). They occur rarely as planes of secondary inclusions along healed fractures. Many of the carbonic inclusions appear to have decrepitated.

*$H_2O$-$CO_2$ inclusions:* These inclusions consist of two (liquid water + dominantly liquid $CO_2$) or three (liquid water + $CO_2$-rich liquid + $CO_2$-rich vapor) phases at 20°C (Fig. 8b-c). The volumetric percentages of the carbonic ($CO_2$ + $CH_4$) components (liquid + vapor) at 20°C vary typically from 10 to 60 percent in individual samples. Some clusters of $H_2O$-$CO_2$ inclusions show a greater variance in the volumetric percentages of the carbonic phases (10–80%) and have $CO_2$-rich inclusions associated with them. $H_2O$-$CO_2$ inclusions occur as isolated inclusions and in random three-dimensional patterns, likely indicating a primary or pseudosecondary origin. These inclusions (10–25 $\mu$m) are typically larger than and are rarely associated with aqueous inclusions (typically <10 $\mu$m; Fig. 8c). $H_2O$-$CO_2$ inclusions are relatively rare and are found dominantly in early quartz-carbonate veins that contain small amounts of clear, microcrystalline quartz, indicating that, in the ore zones, these inclusions are early and predate vein deformation and recrystallization.

*Aqueous inclusions:* These inclusions consist of one ($H_2O$-rich liquid) or two ($H_2O$-rich liquid + vapor) phases. Rare, single-phase aqueous inclusions occur in stage III carbonates and less frequently in stage II carbonates. They are present as isolated inclusions and as inclusions distributed along growth planes, indicating a primary and/or pseudosecondary origin. Many of the inclusions along growth planes have highly irregular shapes and appear to have necked.

Two-phase aqueous inclusions occur in three-dimensional clusters and as randomly distributed, isolated inclusions in stage II vein calcite and less frequently in stage III calcite and dolomite. They vary from highly irregular to negative crystal shapes. In stage I quartz, two-phase aqueous inclusions occur dominantly as secondary inclusions along healed fractures (Fig. 8d). They occur rarely in small three-dimensional clusters that locally cross grain boundaries. Vapor bubbles in the two-phase inclusions comprise 5 to 15 percent of the inclusion volumes.

### *Heating and freezing data*

*Stage I veins:* Carbonic inclusions in stage I quartz-carbonate veins contain solid $CO_2$ and vapor when cooled to approximately –97°C. Upon heating, the first melting of the solid occurs near –70°C. Final melting of the solid $CO_2$ ($T_{m(CO_2)}$ ranges from –65.2° to –56.6°C (Fig. 9a), indicating the presence of variable amounts of $CH_4$ (Burruss, 1981a, b). The carbonic inclusions fall into two groups with low and moderate $CH_4$ contents ($X_{CH_4}$ = 0.00–0.09 and 0.10–0.49). Homogenization of $CO_2$ ($T_{h(CO_2)}$) to the liquid phase occurs between –30.2 and +30.1°C (only 33 of 204 $T_{h(CO_2)}$ values are

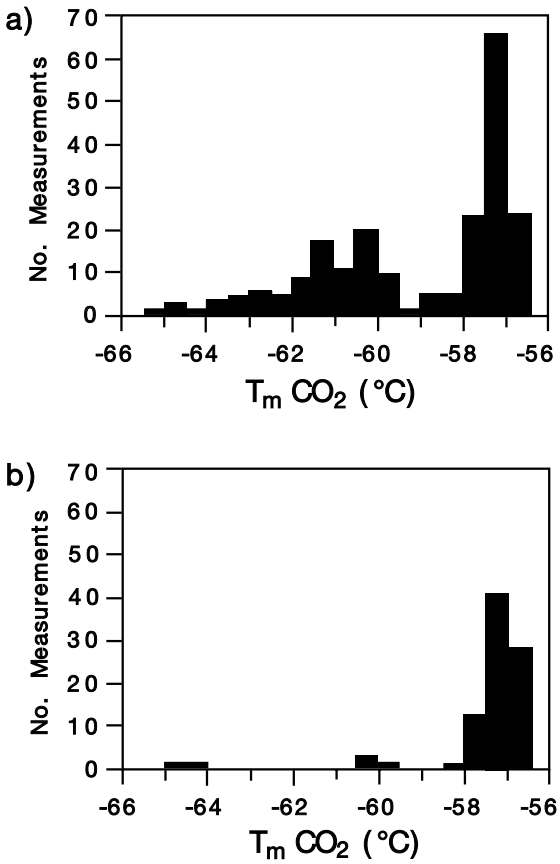


FIG. 9. Frequency diagrams of melting temperatures of $CO_2$ for (a) carbonic and (b) $H_2O$-$CO_2$ fluid inclusions.

<–4.0°C, Fig. 10a), corresponding to $CO_2$(±$CH_4$) densities of 0.59 to 1.08 g/cm$^3$. Two-thirds of the inclusions with $T_{h(CO_2)}$ values <–4.0°C (i.e., the more dense inclusions) have high $CH_4$ contents ($X_{CH_4}$ = 0.12–0.48). The high variability of $T_{h(CO_2)}$ values, even in individual samples, may indicate that the density of the $CO_2$-rich phase was highly variable during entrapment, possibly caused by pressure fluctuations, or that postentrapment leakage and partial decrepitation occurred (cf. Roedder, 1984; Hollister, 1990; Craw and Norris, 1993; Johnson and Hollister, 1995).

Values for $T_{m(CO_2)}$ range from –58.0° to –56.6°C for most $H_2O$-$CO_2$ inclusions, indicating nearly pure $CO_2$ (Fig. 9b). Six of the 88 inclusions measured have $T_{m(CO_2)}$ values between –64.8° and –60.0°C, indicating up to 0.41 $X_{CH_4}$ in the carbonic phase. The $CO_2$-rich phase homogenizes to the liquid between –12.4° and +29.5°C and to the vapor between 16.5° and 30.3°C (Fig. 10b). Bulk densities of $H_2O$-$CO_2$ inclusions range from 0.69 to 1.08 g/cm$^3$. Clathrate melting temperatures ($T_{m(clathrate)}$)range from –4.6° to +13.0°C. These values correspond to salinities ranging from 19.4 to 2.8 wt percent NaCl equiv, respectively (Diamond, 1992; Brown and Hagemann, 1995). $H_2O$-$CO_2$ inclusions homogenize to vapor ($n$ = 4) and liquid ($n$ = 55) over the intervals 370° to 410° and 184° to 360°C, respectively (Fig. 11). Many $H_2O$-$CO_2$ inclusions decrepitated in the range of 140° to 314°C during heating, prior to homogenization.

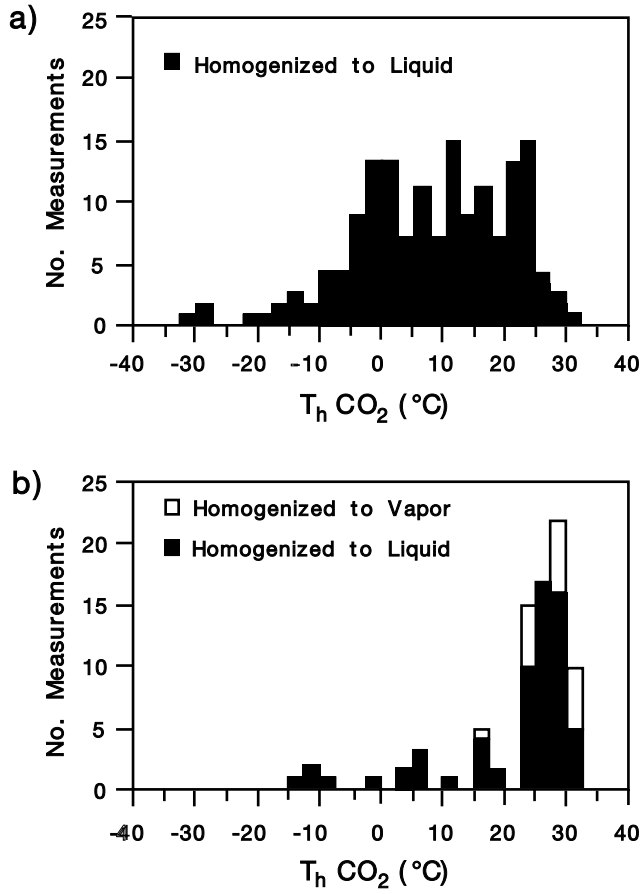


FIG. 10. Frequency diagrams of homogenization temperatures of $CO_2$ for (a) carbonic and (b) $H_2O$-$CO_2$ fluid inclusions.

Eutectic melting temperatures ($T_e$) in secondary, aqueous inclusions were observed between –65° and –40°C (most between –60° and –50°C), although only a few measurements could be made because of the extreme difficulty in detecting the first appearance of liquid. These measurements indicate that the major dissolved salts in the aqueous inclusions are NaCl and $CaCl_2$ (Crawford, 1981; Zhang and Frantz, 1989). Final ice melting temperatures ($T_m$) of secondary, aqueous inclusions in stage I veins range from –42.7° to –10.2°C, indicating highly variable salinities with none less than 14 wt percent NaCl equiv (Fig. 11). These aqueous, NaCl-$CaCl_2$ brine inclusions homogenize to the liquid between 90° and 251°C, with 86 percent of the data between 100° and 160°C (Fig. 11).

*Stage II veins:* The number of aqueous fluid inclusions analyzed from stage II carbonates was limited by the dark, finely crystalline nature of the vein calcite. $T_m$ values ($n$ = 3) range from –32.2° to –36.1°C and $T_h$ values ($n$ = 7) range from 72° to 273°C (mean, 160°C).

*Stage III veins:* Most single-phase, primary aqueous inclusions failed to nucleate vapor bubbles during freezing measurements. Some one-phase aqueous inclusions nucleated a small bubble, comprising ~5 percent of inclusion volume, upon freezing and thawing. Their $T_h$ values are reported with the data for two-phase aqueous inclusions. Two-phase aqueous inclusions in stage III vug-filling calcites and dolomites homogenize to the liquid at temperatures of 95° to 115°C. $T_m$ values range from –3.7° to +4.0°C, corresponding to salinities <6.0 wt percent NaCl (Zhang and Frantz, 1989; Bodnar and Vityk, 1994). Positive $T_m$ values likely indicate the presence of metastable superheated ice (Roedder, 1984).

### Interpretation of Fluid Inclusion Data

Four distinct fluid types were trapped in quartz and/or carbonate: (1) a $CO_2$-rich (±$CH_4$) fluid with densities ranging

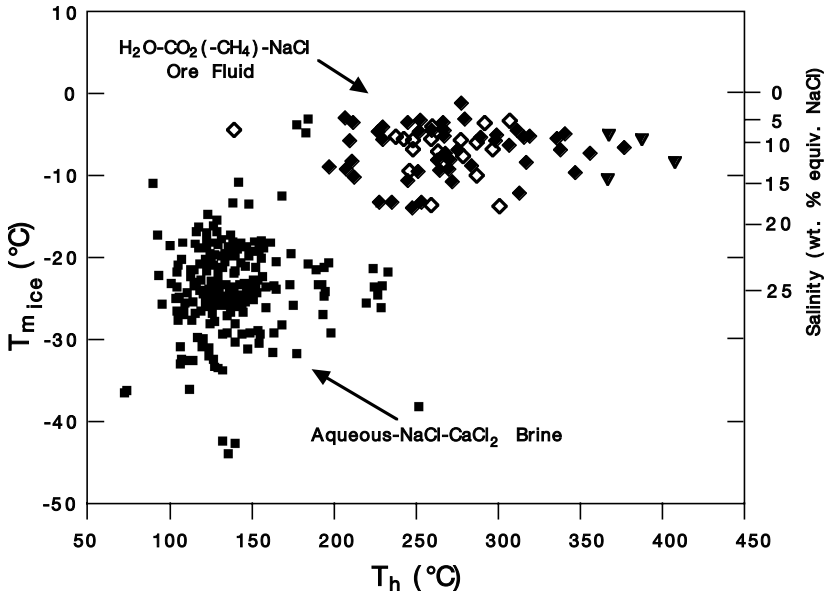


FIG. 11. Homogenization temperature vs. last ice-melting temperature and salinity of aqueous (solid squares) and $H_2O$-$CO_2$ fluid inclusions (solid diamonds = homogenization to liquid, open diamonds = decrepitation, solid triangles = homogenization to vapor).

from 0.59 to 1.08 g/cm$^3$, (2) an$H_2O$-$CO_2$ ($\pm CH_4$) fluid of low to moderate salinity (~3–20 wt % NaCl equiv), (3) anNaCl-$CaCl_2$ aqueous brine of moderate to high salinity ($T_m$ = –42.7° to –10.2°C), and (4) an aqueous fluid of low salinity (<4 wt % NaCl).

*Origin of $CO_2(\pm CH_4)$ fluid inclusions: Distinct fluid, leakage, or unmixing?*

Stage I gold-bearing quartz veins in the Giant mine contain abundant $CO_2$-rich fluid inclusions, with variable densities and comparatively few $H_2O$-$CO_2$ inclusions. $CO_2$-rich fluid inclusions can form by various processes: (1) as a result of postentrapment, deformation-recrystallization processes, such as crystal-plastic deformation and grain-boundary migration recrystallization, that favor trapping of $CO_2$-rich inclusions (Bakker and Jansen, 1990; Hollister, 1990; Craw and Norris, 1993; Johnson and Hollister, 1995); (2) by preferential trapping of $CO_2$ that unmixed from an $H_2O$-$CO_2$ fluid because of the difference in wetting properties between the $CO_2$-rich phase and the aqueous phase (Watson and Brenan, 1987); or (3) by the entrapment of a separate and distinct $CO_2$-rich fluid.

*Distinct fluid versus leakage:* Primary, $CO_2$-rich fluid inclusions with variable densities (0.65–1.06 g/cm$^3$) are also the main type of inclusion found in other mesothermal gold-bearing quartz veins (e.g., the Ashanti mine, Ghana; Schmidt Mumm et al., 1997). At Ashanti, such inclusions were observed forming clusters in euhedral quartz and were interpreted to be the ore-forming fluid. Klemd (1998) disputed this interpretation for the origin of the $CO_2$-rich inclusions in favor of an explanation involving posttrapping, deformation-recrystallization processes during retrograde metamorphism. Klemd's explanation is based on (1) evidence that gold-bearing quartz veins in the Ashanti belt have undergone ductile deformation and recrystallization (Manu, 1993; Klemd et al., 1997); (2) studies showing that ductile deformation (Hollister, 1990) and grain-boundary migration recrystallization favor the entrapment of $CO_2$-rich inclusions and can result in primary, cluster-bound, $CO_2$-rich inclusions (Craw and Norris, 1993; Lamb, 1993; Johnson and Hollister, 1995); and (3) fluid inclusion textures that indicate posttrapping modifications (Klemd et al., 1993, 1997).

In our studies of the Giant mine, textural observations indicate that leakage has occurred and that some $CO_2$-rich inclusions may have formed from earlier mixed $H_2O$-$CO_2$-salt fluid inclusions as a result of later, crystal-ductile deformation and recrystallization. Quartz vein and silicified schist samples, in which the majority of the inclusions are the $CO_2$-rich type, typically contain >30 percent clear, microcrystalline quartz. Medium-grained quartz hosting $CO_2$-rich fluid inclusions has undulose extinction and is surrounded and cut by clear, recrystallized quartz. $CO_2$-rich inclusions characteristically occur in clusters together with infrequent, dark, apparently empty inclusions.

*Unmixing origin?:* Conversely, observations of fluid inclusions from the Giant mine also indicate that some of the $CO_2$-rich inclusions may have formed by unmixing of an $H_2O$-$CO_2$ ore fluid during deposition of stage I vein quartz (using the criteria of Ramboz et al., 1982). The occurrence of $CO_2$-rich and $H_2O$-$CO_2$ inclusions as primary and/or pseudosecondary inclusions in the same stage I veins indicates that they are related. $H_2O$-$CO_2$ inclusions in individual samples have a wide range of $CO_2$ contents and occur in the same clusters and healed fractures as $CO_2$-rich inclusions. $H_2O$-$CO_2$ inclusions containing >60 vol percent $CO_2$ and <40 vol percent $CO_2$ homogenize at similar temperatures to the vapor and liquid phases, respectively.

Most $H_2O$-$CO_2$ fluid inclusions from stage I gold-bearing quartz veins in the Giant mine homogenize between 200° and 300°C (Figs. 11–12). Solvi for the systems $H_2O$-$CO_2$-$CH_4$-6 wt percent NaCl at 1.0 kbar (Danniel et al., 1967) and $H_2O$-$CO_2$-6 wt percent NaCl at 2.0 kbars (Gehrig, 1980) are shown in Figure 12. $H_2O$-$CO_2$-NaCl fluids unmixing between these two solvi, at temperatures of 250° to 350°C, would produce extremely $CO_2$ rich fluids ($X_{CO_2}$ values >0.8) such as those observed in the Giant mine. The majority of $H_2O$-$CO_2$ inclusion compositions fall between these two solvi, further supporting fluid unmixing.

Evidence for fluid unmixing is also seen in gold-bearing quartz veins from metasedimentary rocks 10 to 13 km northeast of Yellowknife, NWT. Primary, $H_2O$- and $CO_2$-rich, $H_2O$-$CO_2$ fluid inclusions homogenize to the liquid and vapor, respectively, from 210° to 322°C (English, 1981).

Variation of densities in $CO_2$-rich fluid inclusions can be caused by pressure fluctuations during fluid entrapment, fluid unmixing, and leakage (Roedder, 1984). The carbonic inclusions in the Giant mine have a wide range of densities (0.59–1.08 g/cm$^3$) that may reflect these processes. However, it is impossible to determine unequivocally the cause of the $CO_2$ density variations.

Based on the evidence presented by fluid inclusions in gold-bearing quartz veins at Giant, both fluid unmixing and posttrapping deformation-recrystallization processes are most likely responsible for the $CO_2$-rich fluid inclusions. The extent and significance of unmixing is difficult to determine because of the scarcity of primary $H_2O$-$CO_2$ fluid inclusions and the paucity of gold-bearing quartz veins showing limited recrystallization.

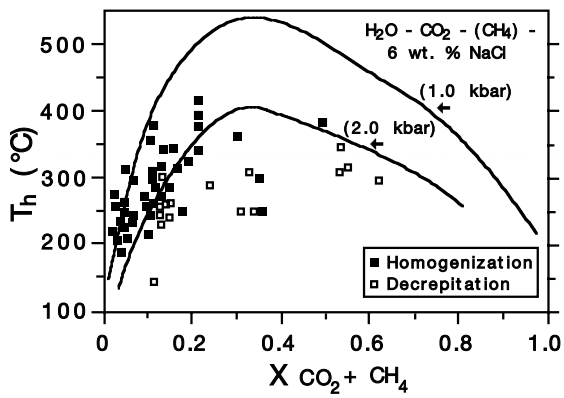


FIG. 12. Bulk composition vs. homogenization temperature diagram, showing relationships between estimated compositions of $H_2O$-$CO_2$ fluid inclusions and immiscibility solvi for $H_2O$-$CO_2$.($CH_4$)-6 wt percent NaCl systems at different pressures. Data sources: 1.0-kbar curve from Danniel et al. (1967), 2.0-kbar curve from Gehrig (1980).

*Origin of $H_2O$-$CO_2$ fluid inclusions*

The majority of $H_2O$-$CO_2$ fluid inclusions were found in stage I quartz veins, infrequently containing free gold. The relationship between salinity and $X_{CO_2}$ for $H_2O$-$CO_2$ fluid inclusions is shown in Figure 13. For inclusions with $X_{CO_2}$ values between 0.2 and 0.6 there is an apparent trend of increasing salinity with increasing water content. This trend supports our earlier suggestion that some unmixing of the $H_2O$-$CO_2$-NaCl fluid occurred, as salt will fractionate preferentially into the aqueous phase during unmixing (Bowers and Helgeson, 1983).

Fluid inclusions with $X_{CO_2}$ <0.2 exhibit a wide range of salinities from 4 to 18 wt percent NaCl equiv. We speculate that inclusions with salinities >10 wt percent NaCl equiv represent remnant aqueous fluids following unmixing. Bowers and Helgeson (1983) have shown that high-salinity $H_2O$-rich fluids can be produced from unmixing of a relatively low salinity $H_2O$-$CO_2$ fluid, because nearly all of the salt will partition into the $H_2O$-rich liquid phase rather than into the $CO_2$-rich vapor phase. Those with $X_{CO_2}$ values of 0.05 to 0.20 and salinities between 4 and 9 wt percent NaCl equiv are thought to be indicative of the parent fluid that did not unmix. Such a $H_2O$-$CO_2$-NaCl fluid composition is similar to those documented in other Precambrian greenstone-hosted gold deposits (Robert and Kelly, 1987; Kerrich and Fyfe, 1988; Kerrich and Kamineni, 1988; Kesler, 1991; Ho et al., 1992; Samson et al., 1997; Shelton et al., 2000) and in orogenic mesothermal systems (Shelton et al., 1988; So et al., 1995; Groves et al., 1998; Jia et al., 2003).

*Pressure-temperature considerations for $H_2O$-$CO_2$ fluid inclusions*

It is a precarious matter to estimate the pressures and temperatures of fluid entrapment using fluid inclusions formed by unmixing (Roedder and Bodnar, 1980). Homogenization temperatures of immiscible, $H_2O$- and $CO_2$-rich, $H_2O$-$CO_2$ inclusions correspond to the entrapment temperatures of these fluids. Most $H_2O$-$CO_2$ fluid inclusion compositions from the Giant mine fall between solvi for the system $H_2O$-$CO_2$ (-$CH_4$)-6 wt percent NaCl at 1.0 (Danniel et al., 1967) and 2.0 kbars (Gehrig, 1980) at temperatures of 250° to 350°C (Fig. 12). Estimated pressures correspond to minimum depths of ~3 to 7 km, assuming purely lithostatic pressure (and were likely deeper, as evidence of fracturing and fluid movement imply a hydrostatic component to the pressure regime). These pressures and temperatures estimated from unmixed inclusions apply only to ore in stage I veins and are in good agreement with P-T conditions suggested for the formation of other large gold systems (Hodgson et al., 1993).

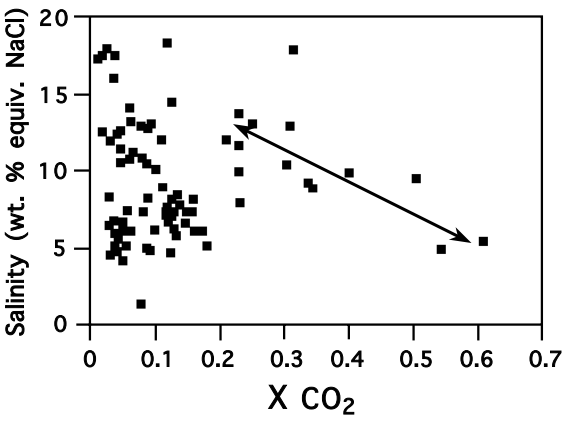


FIG. 13. $X_{CO_2}$ vs. salinity diagram for $H_2O$-$CO_2$ fluid inclusions. Note increasing salinity with increasing water content for fluid inclusions with $X_{CO_2}$ values between 0.2 and 0.6 (line with arrows; R = 0.71) and the wide range of salinities for inclusions with $X_{CO_2}$ <0.2.

Temperature and pressure determinations for refractory, wall-rock–hosted ores in the Yellowknife greenstone belt are limited by the lack of key geobarometric mineral assemblages and the scarcity of reliable, primary fluid inclusions. Chary (1971) estimated a temperature range of 300° to 350°C for mineralization in the nearby Con mine (Fig. 1), based on fluid inclusion homogenization temperatures and sulfur isotope partitioning between sulfide pairs. Armstrong (1997) calculated mineralization temperatures of 300° to 420°C for refractory ore zones and temperatures of less than 375°C for free-milling, native gold ores in the Con mine, using arsenopyrite and chlorite geothermometry. Calculated oxygen isotope temperatures of gold-bearing quartz veins from the Campbell shear zone are 270° to 380°C (Kerrich and Fyfe, 1988).

*Origin of aqueous-brine fluid inclusions*

Aqueous-brine (NaCl-$CaCl_2$-$H_2O$) inclusions in ore-related (stage I) quartz are found as secondary inclusions in healed fractures and were not found to be associated intimately with $H_2O$-$CO_2$- or $CO_2$-rich fluid inclusions. They have moderate to high salinities ($T_m$ = –42.7° to –10.2°C) and low homogenization temperatures (generally <170°C; Fig. 11). Aqueous fluid inclusions of similar salinity and homogenization temperature occur in the later (stage II) banded and fracture-filling carbonate as apparent primary inclusions.

Reconnaissance gas analysis by quadrupole mass spectrometry of fluid inclusions from stage I quartz vein samples in the extreme western portion of the mine revealed no fluid or very small amounts of water, indicating that ore-related fluid inclusions ($H_2O$-$CO_2$ type) have largely been decrepitated, plausibly by movement along Proterozoic faults and by higher grade metamorphism. These veins have undergone, to some degree, crushing and recrystallization, as indicated by significant amounts of clear, microcrystalline quartz and strained quartz having undulose extinction. In gold-bearing quartz veins adjacent to the Proterozoic West Bay fault, fluid inclusions are scarce, and when found, only secondary, highly saline ($T_m$ = –33.5 to –20.6°C), aqueous inclusions were observed. The NaCl-$CaCl_2$ brine inclusions thus are interpreted to be unrelated to gold deposition and to represent a distinct, postdeformational fluid that infiltrated the greenstone belt.

Secondary, moderately to highly saline, aqueous fluids have also been observed in other parts of the Yellowknife greenstone belt and Slave province: (1) in quartz veins from shear zones on the Mirage Islands, 25 km south of Yellowknife, where the southernmost exposures of the Yellowknife greenstone belt occur (Relf, 1988), (2) in gold-bearing quartz veins from metasedimentary rocks of the Yellowknife Supergroup (10–12 km northeast, 85 km northeast, and 90 km east of Yellowknife; English, 1981), and (3) in gold-bearing quartz veins from the Colomac mine, located 220 km north of Yellowknife

within the Indin Lake supracrustal belt (Costello, 1999; Shelton et al., 2000). In these areas, secondary, aqueous inclusions have $T_h$ values (~110°–170°C) and salinities (>10 wt % NaCl equiv) similar to those for the NaCl-$CaCl_2$ brine inclusions in gold-bearing veins at the Giant mine and have been interpreted to represent a later, postgold hydrothermal fluid moving through fractures. A common origin is supported by the fact that all of these areas have been transected by the Indin-West Bay Proterozoic fault system.

*Low-salinity, aqueous fluid inclusions*

Low-salinity (<7 wt % NaCl equiv), aqueous fluid inclusions are the only type of inclusion found in stage III vug-filling carbonates. They are not observed in any other stage of mineralization and represent a temporally distinct fluid from the gold ore fluid and NaCl-$CaCl_2$ brine.

## Stable Isotope Studies

Samples of quartz ± carbonate and carbonate veins and vug-filling carbonate from underground stopes and drill cores were collected for stable isotope study. See McMenamy (1999) and van Hees et al. (1999) for detailed descriptions and localities for samples listed in Table 1. Locations of quartz samples used to construct the contoured cross section in Figure 4c are given in Table 2.

Oxygen isotope composition of carbonates and quartz, C isotope composition of carbonates, and S isotope composition of sulfides were measured. Quartz was reacted with $ClF_3$

TABLE 1. Stable Isotope Compositions of Vein Minerals

| Sample no. | Mineral | $\delta^{18}O$ (‰) | $\delta^{13}C$ (‰) | $\delta^{18}O_{water}$ (‰)[1] |
|---|---|---|---|---|
| Stage I veins outside main wall-rock alteration zone in Figure 3b | | | | |
| AA1871 | Quartz | 11.1 | | 5.3 |
| AA4804 | Quartz | 9.3 | | 3.5 |
| AA8154 | Quartz | 9.9 | | 4.1 |
| AA8155 | Quartz | 11.4 | | 5.6 |
| AA8159 | Quartz | 9.7 | | 3.9 |
| AA8169 | Quartz | 10.7 | | 4.9 |
| AA8163 | Quartz | 11.4 | | 5.6 |
| AA8173 | Quartz | 10.0 | | 4.2 |
| AA9107 | Quartz | 10.4 | | 4.6 |
| AA9111 | Quartz | 9.0 | | 3.2 |
| AA9124 | Quartz | 11.1 | | 5.3 |
| AB1134 | Quartz | 8.6 | | 2.8 |
| AB1577 | Quartz | 10.7 | | 4.9 |
| AB2128 | Quartz | 10.4 | | 4.6 |
| AB2132 | Quartz | 11.0 | | 5.2 |
| Stage I veins within main wall-rock alteration zone in Figure 3b | | | | |
| 61014 | Quartz | 12.1 | | 6.3 |
| A1 | Quartz | 11.8 | | 6.0 |
| AA1853-g | Quartz | 13.3 | | 7.5 |
| AA1853-w | Quartz | 14.1 | | 8.3 |
| AA1856 | Quartz | 13.8 | | 8.0 |
| AB1126 | Quartz | 11.8 | | 6.0 |
| AB1130 | Quartz | 12.9 | | 7.1 |
| AB1141 | Quartz | 11.9 | | 6.1 |
| AB1146 | Quartz | 13.1 | | 7.3 |
| AB1167 | Quartz | 12.2 | | 6.4 |
| AB1583 | Quartz | 11.5 | | 5.8 |
| Brock Vein | Quartz | 12.9 | | 7.1 |
| Stage I veins not in section a-a' or b-b' of Figure 2 | | | | |
| 7A | Calcite | 16.7 | –2.9 | |
| 622 | Calcite | 11.4 | –3.4 | 7.1 |
| 758 | Calcite | 11.7 | –5.6 | 7.4 |
| 766 | Calcite | 10.9 | –3.9 | 6.6 |
| 837 | Calcite | 14.1 | –1.9 | 9.8 |
| | Quartz | 13.1 | | 7.3 |
| 984 | Calcite | 10.1 | –2.1 | 5.8 |
| | Quartz | 12.1 | | 6.3 |
| 2998 | Calcite | 18.0 | –2.7 | |
| | Quartz | 14.7 | | 9.9 |
| H.S. VG | Calcite | 17.8 | –1.4 | |
| | Quartz | 11.3 | | 5.5 |
| KS96-1 | Calcite | 9.7 | –2.6 | 5.4 |
| | Quartz | 10.8 | | 5.0 |
| KS96-2 | Calcite | 8.6 | –1.6 | 4.4 |
| KS96-3 | Calcite | 9.9 | –1.4 | 5.6 |
| | Quartz | 10.6 | | 4.8 |
| KS96-6 | Calcite | 10.9 | –3.8 | 6.6 |
| KS96-8 | Calcite | 13.8 | –4.3 | 9.5 |
| | Quartz | 11.6 | | 5.8 |
| | Quartz | 12.0 | | 6.2 |
| | Quartz | 11.9 | | 6.1 |
| KS96-9 | Calcite | 10.3 | –1.8 | 6.0 |
| KS96-10 | Calcite | 11.0 | –4.7 | 6.8 |
| Stage II banded calcite and late fracture-filling calcite in stage I veins | | | | |
| 563 | Calcite[2] | 22.5 | –1.7 | 10.6 |
| 825 | Calcite[2] | 24.0 | –1.8 | 12.1 |
| 911 | Calcite[2] | 20.6 | –4.4 | 8.7 |
| 3631 | Calcite[2] | 26.1 | –2.5 | 14.1 |
| KS96-11A | Calcite[3] | 23.3 | –3.7 | 11.3 |
| KS96-14A | Calcite[3] | 23.3 | –3.8 | 11.3 |
| KS96-14C | Calcite[3] | 23.6 | –4.2 | 11.6 |
| KS96-14D | Calcite[3] | 22.4 | –4.3 | 10.5 |
| Stage III vug-filling carbonates | | | | |
| KS96-11B | Dolomite | 15.8 | –3.7 | –4.6 |
| KS96-14B | Red Calcite | 17.2 | –5.1 | 1.2 |
| KS96-14E | Dolomite | 13.4 | –4.7 | –6.9 |
| KS96-15A | Dolomite | 16.4 | –4.0 | –3.9 |
| KS96-15B | Calcite | 10.9 | –9.1 | –5.1 |
| KS96-16 | Dolomite | 15.8 | –4.0 | –4.5 |
| KS96-17 | Dolomite | 15.5 | –4.2 | –4.9 |
| KS97-1A | Dolomite[4] | 17.4 | –4.1 | –2.9 |
| | Dolomite[5] | 14.3 | –5.4 | –6.0 |
| KS97-1B | Dolomite[4] | 17.2 | –4.0 | –3.1 |
| | Dolomite[5] | 14.1 | –5.1 | –6.2 |
| KS97-2 | Black calcite | 17.7 | -4.8 | 1.7 |

Notes: The quartz data in this table are from van Hees et al. (1999) and were used to construct Figure 3c; we have utilized them here to calculate $\delta^{18}O_{water}$ values

[1] Calculated from the quartz-water curve of Clayton et al. (1972) at 350°C and the calcite-water curve of O'Neil et al. (1969) at 350°C (stage I), 160°C (stage II), and 110°C (stage III)

[2] Fracture-filling

[3] Banded

[4] Core

[5] Rim

TABLE 2. Stable Isotope Compositions of Vein Quartz from Thick Section b-b' in Figures 2 and 4b

| Sample no. | $\delta^{18}O$ (‰) | Drill hole/ location | Depth (ft) | Easting (ft) | Northing (ft) | Elevation (ft) | Host rock |
|---|---|---|---|---|---|---|---|
| 537 | 9.2 | S973 | 16 | 2,308.7 | –2,105.0 | 6,036.2 | Tuff |
| 554 | 13.4 | 5846 | 666 | 2,580.5 | –2,632.8 | 4,065.2 | Graywacke |
| 622 | 10.9 | S-1955 | 2,474 | 1,774.3 | –2,218.3 | 3,738.7 | Massive flow |
| 701 | 10.8 | Surface | | 1,700.0 | –2,900.0 | 6,100.0 | Pillow basalt |
| 703 | 12.0 | Surface | | 3,150.0 | –2,300.0 | 6,100.0 | Massive basalt |
| 710 | 9.3 | Surface | | 2,120.0 | –2,300.0 | 6,100.0 | Massive basalt |
| 715 | 11.0 | Surface | | 1,000.0 | –2,600.0 | 6,100.0 | Variolitic pillow flow |
| 719 | 12.5 | Surface | | –150.0 | –3,020.0 | 6,100.0 | Pillow basalt |
| 722 | 11.2 | Surface | | –850.0 | –2,800.0 | 6,100.0 | Pillow basalt |
| 724 | 10.9 | Surface | | 100.0 | –2,900.0 | 6,100.0 | Shear zone |
| 753 | 11.3 | S-1857 | 688 | –531.1 | –3,232.0 | 5,433.6 | Massive flow |
| 771 | 10.4 | S-1857 | 3,593 | 458.2 | –3,123.6 | 2,707.8 | Mafic flow |
| 778 | 10.8 | S-1857 | 4,562 | 888.4 | –3,047.3 | 1,843.7 | Mafic flow |
| 785 | 9.2 | 13193 | 279 | 586.9 | –2,918.3 | 4,912.2 | Greenstone |
| 803 | 10.2 | 12263 | 170 | 285.0 | –3,035.3 | 4,937.4 | Greenstone |
| 810 | 11.8 | 11712 | 454 | 529.8 | –1,474.8 | 3,625.8 | Massive flow |
| 815 | 11.9 | 11712 | 1,455 | 1,270.4 | –1,377.3 | 3,004.7 | Chlorite schist |
| 837 | 13.0 | 11100 | 2,465 | 2,645.3 | –1,376.6 | 3,466.7 | Variolitic pillow flow |
| 840 | 11.8 | 11100 | 1,805 | 1,986.2 | –1,376.6 | 3,501.3 | Chlorite schist |
| 842 | 11.7 | 11100 | 1,467 | 1,648.7 | –1,376.6 | 3,519.2 | Pillow flow |
| 844 | 11.2 | 11100 | 285 | 541.1 | –1,482.0 | 3,844.5 | Gabbro |
| 849 | 11.0 | 11100 | 736 | 939.6 | –1,454.3 | 3,640.0 | Chloritic metagabbro |
| 865 | 11.0 | 20701 | 477 | 754.3 | –1,986.5 | 4,095.0 | Massive flow |
| 874 | 10.2 | 20701 | 2,670 | 1,745.9 | –1,316.8 | 2,304.5 | Massive flow |
| 876 | 10.7 | 20701 | 1,545 | 1,197.7 | –1,809.3 | 3,145.2 | Variolitic pillow flow |
| 906 | 11.0 | 5366 | 350 | 3,191.7 | –1,189.7 | 4,381.7 | Graywacke |
| 910 | 9.9 | 5366 | 40 | 3,155.9 | –1,189.4 | 4,088.5 | Graywacke |
| 911 | 13.3 | 6300 | 35 | 1,852.6 | –1,186.1 | 4,002.9 | Greenstone |
| 916 | 12.3 | 6300 | 1,076 | 2,228.5 | –1,026.3 | 3,088.3 | Greenstone |
| 931 | 10.4 | 5470 | 1,045 | 2,768.1 | –1,191.2 | 3,114.8 | Greenstone |
| 939 | 12.7 | 5470 | 1,549 | 3,189.2 | –1,198.5 | 2,843.5 | Quartzite |
| 981 | 12.0 | S-974 | 922 | 2,498.6 | –2,459.1 | 5,466.8 | Greenstone |
| 984 | 12.1 | S-974 | 82 | 1,962.0 | –2,124.6 | 6,009.0 | Metagabbro |
| 1000 | 10.6 | 19269 | 944 | 979.7 | –2,688.1 | 5,422.0 | Pillowed flow |
| 2978 | 11.0 | S-1955 | 3,528 | 1,272.5 | –2,193.6 | 2,817.4 | Massive flow |
| 2984 | 10.4 | S-1955 | 4,350 | 755.6 | –2,050.8 | 2,196.2 | Pillow flow |
| 2986 | 11.6 | S-1955 | 75 | 2,618.2 | –1,911.3 | 5,961.4 | Chlorite schist |
| 2992 | 11.6 | S-1955 | 953 | 2,332.4 | –2,040.9 | 5,141.5 | Metagabbro |
| 2997 | 12.8 | 25660 | 218 | 897.5 | –2,430.8 | 4,544.4 | Metagabbro |
| 2998 | 14.6 | 25560 | 815 | 1,482.2 | –2,530.4 | 4,537.9 | Chlorite-sericite schist |
| 2999 | 11.9 | 25560 | 1,174 | 1,829.0 | –2,622.5 | 4,548.3 | Mafic volcanics |
| 3000 | 10.4 | 2556 | 27 | 707.2 | –2,423.1 | 4,545.0 | Gabbro |
| 3607 | 10.6 | 19269 | 148 | 290.4 | –2,290.1 | 5,422.0 | Chlorite schist |
| 3608 | 12.0 | 19269 | 1,438 | 1,407.6 | –2,935.1 | 5,422.0 | Pillow flow |
| 3623 | 12.2 | 6300 | 1,861 | 2,908.1 | –967.7 | 2,728.1 | Greenstone |
| 3631 | 10.5 | S-1854 | 559 | 798.8 | –2,713.3 | 5,503.1 | Massive flow |
| 3638 | 10.6 | S-1854 | 1,542 | 893.2 | –2,738.1 | 4,525.0 | Massive flow |
| 3643 | 9.3 | S-1854 | 2,257 | 968.5 | –2,700.5 | 3,815.4 | Massive flow |
| 3650 | 10.1 | S-1854 | 3,515 | 1,236.4 | –2,513.9 | 2,603.1 | Massive flow |
| 3656 | 11.9 | S-1854 | 4,520 | 1,534.4 | –2,313.9 | 1,664.7 | Massive flow |
| 3668 | 12.0 | 12800 | 35 | 410.8 | –2,818.8 | 5,062.0 | Pillow flow |

Note: Samples located relative to mine grid

using a modification of the Clayton and Mayeda (1963) method. Standard techniques for extraction and analysis of C and S were used, as described by McCrea (1950) and Grinenko (1962). Isotopic data are reported in standard $\delta$ notation relative to Vienna standard mean ocean water (V-SMOW) for oxygen, the Pee Dee belemnite (V-PDB) standard for carbon, and the Cañon Diablo troilite (CDT) standard for sulfur (Tables 1–3, Figs. 14–16). The standard error of each analysis is ±0.2 per mil for $\delta^{18}O$ and <±0.1 per mil for $\delta^{13}C$ and $\delta^{34}S$.

### *Oxygen and carbon isotope study*

*Stage I quartz:* The $\delta^{18}O$ values of stage I vein quartz (36 samples from van Hees et al., 1999, Table 1; 51 samples from this study, Table 2) range from 8.6 to 14.7 per mil (Fig. 15a). Quartz veins hosted within an east-dipping wall-rock alteration zone (van Hees et al., 2004) connecting the Giant ore deposits to the Yellowknife River fault zone to the east have $\delta^{18}O$ values that decrease systematically from 14.7 per mil in deeper metasedimentary rocks toward 11.6 per mil in shallower

TABLE 3. Sulfur Isotope Compositions of Sulfide Minerals

| Stage | Sample no. | Mineral | $\delta^{34}S$ (‰) |
|---|---|---|---|
| I | 61014B | Sphalerite | 4.9 |
| | G7prospect | Pyrite | 9.0 |
| | | Sphalerite | 0.5 |
| | KS96-6 | Bladed stibnite in quartz | 4.3 |
| | KS96-8 | Massive stibnite | –1.4 |
| | KS96-10 | Pyrite | 1.0 |
| | | Chalcopyrite | 1.5 |
| II | KS96-13 | Stibnite | 2.6 |
| | KS96-14 | Galena | 1.3 |
| | | Sphalerite | –5.6 |
| | | Banded pyrite | –0.4 |
| III | KS96-14 | Late stibnite with dolomite | –12.2 |
| | | | –19.5 |
| | KS96-16 | Late stibnite in vug | –21.4 |

metabasalts in the mine (Figs. 3c, 4c). This decrease is interpreted to indicate that $^{18}O$-enriched ore fluids originated in deeper, metasedimentary rocks and reacted extensively with wall rocks along the entire extent of their flow paths before depositing gold dominantly in more $^{16}O$-enriched, shallower, Ti rich tholeiitic metabasalts (van Hees et al., 1999).

Quartz veins, infrequently containing free gold, hosted in metavolcanic rocks outside of the alteration zone have lower $\delta^{18}O$ values (8.6–11.4‰; Table 1, Fig. 3c) than quartz veins within the alteration zone. Utilizing temperature estimates from fluid inclusions (350°C) and the fractionation equation of Clayton et al. (1972), calculated equilibrium $\delta^{18}O_{water}$ values of quartz-depositing fluids outside of the alteration zone are 2.8 to 5.6 per mil and those of quartz-depositing fluids within the alteration zone are 5.8 to 8.3 per mil (Fig. 15b). The difference in ranges of $\delta^{18}O_{water}$ values may indicate that multiple events were responsible for quartz veining and/or that fluids depositing veins outside and inside the alteration zone represent distinct reservoirs that evolved through reaction with isotopically distinct rocks in their source regions (i.e., $^{16}O$-enriched metavolcanic rocks vs. $^{18}O$-enriched metasedimentary rocks).

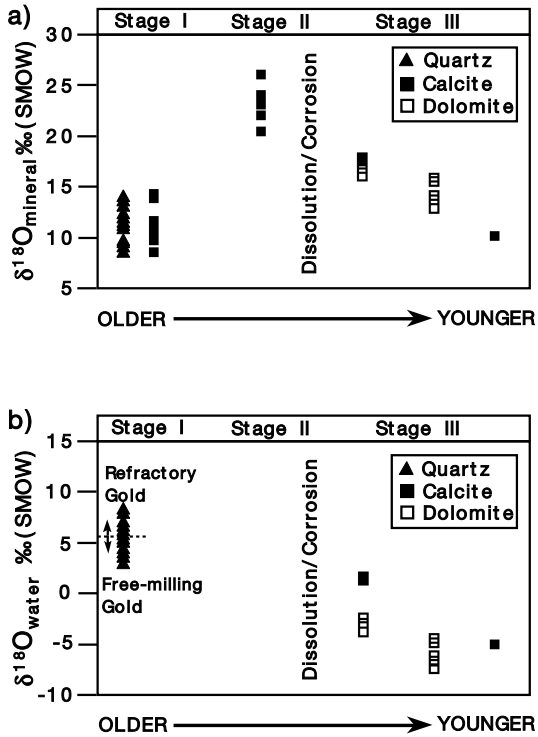


FIG. 15. Vein mineral paragenesis vs. $\delta^{18}O$ values of (a) minerals and (b) calculated equilibrium waters. See Table 1 for data and calculations.

Could gold-bearing quartz veins outside of the main alteration zone represent a separate mineralizing event whose fluids and ore-forming constituents were derived solely from within the metavolcanic rocks? As suggested by van Hees et al. (1999), isotopically, they could. Primary tholeiitic basalts have $\delta^{18}O$ values of 5.7 ± 0.3 per mil (Taylor, 1968; Anderson et al., 1971; Kyser et al., 1981, 1982). Spilitized basalts have higher $\delta^{18}O$ values (e.g., 8.0–10.0‰ in the Dome mine area, Abitibi belt, Kerrich, 1987). Unmineralized metabasalts in the Yellowknife area have $\delta^{18}O$ values of 7.0 to 7.7 per mil (Kerrich and Fyfe, 1981). At a temperature of 400°C, based on fluid inclusion and stable isotope thermometry, ore fluids

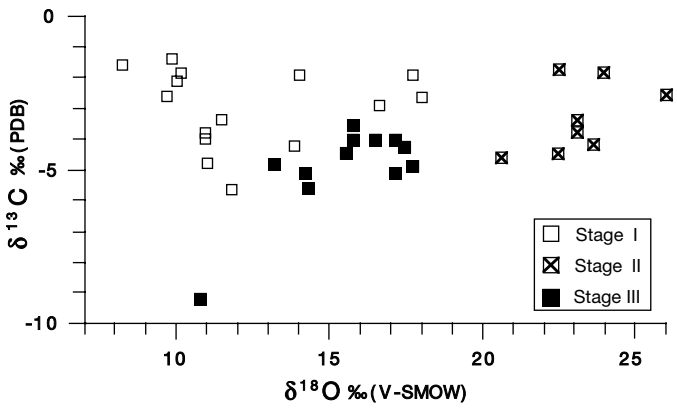


FIG. 14. $\delta^{13}C$ vs. $\delta^{18}O$ diagram for carbonate minerals from various stages of mineralization in the Giant mine.

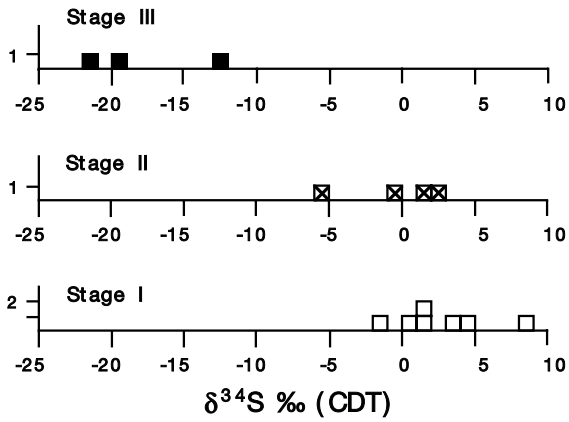


FIG. 16. Frequency diagram of $\delta^{34}S$ values for sulfides from various stages of mineralization in the Giant mine.

in isotopic equilibrium with any of these rocks (O'Neil and Taylor, 1967; Matsuhisa et al., 1979) could have $\delta^{18}O_{water}$ values of 2.8 to 5.6 per mil, like those calculated for fluids depositing gold-bearing quartz veins outside of the alteration zone.

In contrast, gold-bearing quartz veins within the refractory ore-related, wall-rock alteration zone indicate deposition from fluids ($\delta^{18}O_{water}$ = 4.4–9.8‰) that equilibrated with more $^{18}O$-enriched rocks, likely both metavolcanic and metasedimentary. We are unaware of whole-rock $\delta^{18}O$ values of unaltered metasedimentary rocks in the Yellowknife area. However, host-rock quartz in metagraywacke from the nearby Ptarmigan mine has a $\delta^{18}O$ value of 13.9 per mil (Kerrich and Fyfe, 1987). Ore fluids in isotopic equilibrium with similar metasedimentary rocks at temperatures of 350° to 400°C (Clayton et al., 1972) would have $\delta^{18}O_{water}$ values >8 per mil, like those calculated for gold-bearing quartz veins within the refractory ore-related, wall-rock alteration zone.

*Stage I calcite:* The $\delta^{18}O$ and $\delta^{13}C$ values of 12 samples of stage I calcites range from 8.6 to 14.1 and –5.6 to –1.4 per mil, respectively (Figs. 14–15a). Using the calcite-water oxygen isotope fractionation equation of O'Neil et al. (1969) and temperature estimates from fluid inclusions in coexisting quartz (350°C), calculated equilibrium $\delta^{18}O_{water}$ values are 4.4 to 9.8 per mil (Fig. 15b), similar to the range calculated for stage I quartz.

Three stage I calcites have similar $\delta^{13}C$ values (–2.9 to –1.4‰) but higher $\delta^{18}O$ values (16.7–18.0‰) than other stage I calcites. Anomalously high $\delta^{18}O_{calcite}$ values (>16‰) have also been reported in shallow portions of the Con mine and are interpreted to represent reequilibration with surface waters or post-Archean brines at lower temperatures (Kerrich, 1989; Webb, 1992).

*Stage II calcite:* The isotopic compositions of eight samples of stage II calcites were analyzed, four from banded carbonate veins and four from calcite-filled fractures in earlier quartz veins. The $\delta^{18}O$ values of these calcites are 20.6 to 26.1 per mil; their $\delta^{13}C$ values are –4.4 to –1.7 per mil (Figs. 14–15a). Using a fluid inclusion temperature estimate of 160°C and the fractionation equation of O'Neil et al. (1969), calculated equilibrium $\delta^{18}O_{water}$ values are 8.7 to 14.2 per mil (Fig. 15b).

*Stage III dolomite and calcite:* Ten samples of stage III carbonates were analyzed for their isotopic compositions. The earliest carbonates (a red-brown calcite veinlet and black calcite: Fig. 7) have $\delta^{18}O$ values of 17.2 and 17.7 per mil and $\delta^{13}C$ values of –5.1 and –4.8 per mil, respectively (Fig. 14). The cores and edges of two large (2-cm) stage III dolomite crystals were sampled for isotope analysis. The cores have higher $\delta^{18}O$ (17.4 and 17.1‰) and $\delta^{13}C$ values (–4.1 and –4.0‰) than the edges ($\delta^{18}O$ = 14.3 and 14.1‰; $\delta^{13}C$ = –5.4 and –5.1‰, Fig. 14). The $\delta^{18}O$ values of five other stage III vug-filling, clear dolomites range from 13.4 to 16.4 per mil; their $\delta^{13}C$ values range from –4.7 to –3.7 per mil (Fig. 14). The latest stage III carbonate, scalenohedral calcite overgrowing earlier vug-filling dolomite, has the lowest $\delta^{18}O$ (10.9‰) and $\delta^{13}C$ values (–9.1‰; Fig. 15a).

Stage III calcites and dolomites show a systematic trend toward lower $\delta^{18}O$ and $\delta^{13}C$ values with decreasing relative age (Figs. 14–15a). Using the fractionation equation of O'Neil et al. (1969) and a fluid inclusion temperature estimate of 110°C, calculated equilibrium $\delta^{18}O_{water}$ values decrease from +1.1 toward –6.8 per mil with decreasing age (Fig. 15b).

*Sulfur isotope study*

The $\delta^{34}S$ values of 14 samples of sulfide minerals were determined: seven from stage I, four from stage II, and three from stage III (Table 3, Fig. 16). Stage I $\delta^{34}S$ values are 1.0 and 9.0 per mil for pyrite, 0.5 and 4.9 per mil for sphalerite, 1.5 per mil for chalcopyrite, and –1.4 (bladed) and 4.3 per mil (massive) for stibnite. For comparison, Wanless et al. (1960) reported $\delta^{34}S$ values of composite sulfide samples from the Giant mine of 2.4 to 3.6 per mil for pyrite and 0.4 per mil for sphalerite.

Stage II $\delta^{34}S$ values are –0.4 per mil for pyrite, –5.6 per mil for sphalerite, 1.3 per mil for galena, and 2.6 per mil for stibnite (Fig. 16). The $\delta^{34}S$ values of one galena and a composite (stibnite + minor sulfides) sample, reported by Wanless et al. (1960) to be second-stage, postore sulfides, are 0.0 and 0.3 per mil, respectively.

Stage III stibnite associated with large, clear dolomite crystals in vugs has $\delta^{34}S$ values that are much lower (–12.2 to –21.4‰) than earlier gold-bearing ore-related stibnite (+4.3 to –1.4‰).

The much lower $\delta^{34}S$ values of stage III stibnite could represent a sulfur source distinct from that responsible for gold-bearing ore-related stage I stibnite. If the stage III fluids were reducing and $H_2S$ was the dominant sulfur species present, the $\delta^{34}S$ values near –20 per mil would indicate sulfur from a bacteriogenic source, possibly sedimentary pyrite. If stage III fluids remobilized stage I sulfur ($\delta^{34}S$ ~0‰), the low $\delta^{34}S$ values of stage III stibnites would indicate partitioning of $^{34}S$ into dissolved sulfate in a fluid with an $SO_4^{2-}/H_2S$ ratio of ~1 (Sakai, 1968).

## Summary of Isotopically and Chemically Distinct Fluids

The stable isotope data demonstrate that chemically and isotopically distinct fluids were responsible for the three stages of mineralization in the Giant hydrothermal system.

*Ore-related stage I*

The chemical and isotopic evidence for refractory, wall-rock– and high-grade, vein-hosted gold ore at the Giant mine supports a metamorphic origin for their ore fluids. Ore fluids most likely originated during 2.60 to 2.57 Ga (Isachsen and Bowring, 1994) regional metamorphism of the Yellowknife greenstone belt, due to metamorphic dehydration of metavolcanic and metasedimentary rocks (Kerrich, 1989). Although the ore fluids are both metamorphic, are the high-grade, quartz-bearing gold veins the result of the same ore fluids that deposited refractory gold ores or do they represent distinct ore fluids and mineralizing events? If they represent distinct ore fluids and mineralizing events, we might expect to find geochemical differences (fluid inclusion compositions, $\delta^{18}O$ values of quartz) between ore fluids that originated in the metavolcanic rocks and those that originated in metasedimentary rocks. If the veins are part of the same fluid system that deposited refractory gold ores, the differences in style of gold ore mineralization (free-milling vs. refractory) may reflect differences in the extent of chemical interaction of the

ore fluids with wall rocks and/or different mechanisms of ore deposition.

For example, at the nearby Con mine (Fig. 1), varying degrees of fluid–wall-rock reaction, as recorded by distinct chemical compositions of white micas, are associated with different styles of gold ores. Refractory ores deposited at low fluid/rock ratios are typified by aluminous paragonitic micas with minimal substitution of siderophile elements, whereas free-milling ores deposited at high fluid/rock ratios are characterized by muscovite with varying siderophile element substitution (Armstrong, 2002). In contrast, at the Colomac gold mine, 220 km north of Yellowknife, similar fluids formed low-grade, high-tonnage deposits with primarily sulfide-hosted gold as a result of fluid–wall-rock reaction, whereas localized high-grade, gold-bearing quartz vein deposits formed via fluid unmixing (Shelton et al., 2000).

*Refractory, sulfide-hosted ores and gold-bearing quartz veins within the main alteration zone:* Refractory, sulfide-hosted ores and ore-related stage I quartz in the main ore-related wall-rock alteration zone of the Giant mine (Figs. 3, 4) were deposited by $H_2O$-$CO_2$-NaCl fluids at ~300° to 350°C. The $\delta^{18}O$ values of waters depositing this quartz range from 5.8 to 8.3 per mil and are consistent with an $^{18}O$-enriched metamorphic fluid that emerged from the thick metasedimentary sequence to the east and reacted with more $^{16}O$-enriched ore-hosting metavolcanic rocks (van Hees et al., 1999). The values are similar to those reported by Kerrich and Fyfe (1987; $\delta^{18}O_{water}$ = 8.0 ± 0.2‰) for refractory, sulfide-hosted gold ore in the nearby Con mine (van Hees and Shelton, 2002a).

These two styles of gold mineralization appear to be part of the same mineralizing event in which the style of mineralization was dictated by the mechanism of ore deposition. Refractory, sulfide-hosted gold mineralization resulted from reaction of mineralizing fluids with $Fe^{2+}$ in metavolcanic wall rocks. Free-milling, gold-bearing quartz vein ores were deposited as a result of fluid unmixing, with loss of $H_2S$ to the vapor phase.

*Free-milling ores outside of the main wall-rock alteration zone:* Gold-bearing stage I veins outside of the main wall-rock ore-related alteration zone have lower $\delta^{18}O_{water}$ values, ranging from 2.8 to 5.6 per mil. These lower values most likely reflect a metamorphic fluid system dominated by isotopic exchange with metavolcanic rocks. In the nearby Con mine, ore fluids associated with free-milling native gold deposition also have lower $\delta^{18}O_{water}$ values (5.4–6.8‰) than ore fluids associated with refractory sulfide-hosted orebodies (9.1‰; Armstrong, 1997).

Quartz veins outside the main wall-rock alteration zone in the Giant mine were also deposited via fluid unmixing of $H_2O$-$CO_2$-NaCl fluids at ~250° to 350°C, but with isotopically distinct compositions, and need not be related to the sulfide-hosted gold-depositing event. Some of these veins contain abundant sphalerite, indicating that they may have an affinity with the sphalerite-galena gold-depositing event recognized elsewhere in the Yellowknife region by Falck (1992).

### *Postgold ore stage II*

Stage II calcites have higher, relatively uniform $\delta^{18}O$ values (20.6–23.6‰) compared to stage I carbonates and were deposited from a chemically and isotopically distinct fluid at lower temperatures (~160°C). The highly saline fluid responsible for stage II mineralization is interpreted to be an NaCl-$CaCl_2$ brine with anomalously high $\delta^{18}O_{water}$ values of 8.7 to 14.2 per mil.

Fluid inclusion and stable isotope data indicate that the NaCl-$CaCl_2$ brines responsible for stage II mineralization are unrelated to the main gold ore event. A preliminary Pb/Pb model age of ~1250 Ma (Cousens et al., 1999) may indicate that stage II fluids represent a later hydrothermal event not associated with the early (2.6 Ga) regional metamorphism. This later event may instead be related tectonically to widespread basic magmatism in the northwestern Canadian Shield associated with emplacement of the Mackenzie dike swarm at ~1267 Ma (LeCheminant and Heaman, 1989; Frith, 1993).

Saline ground waters encountered deep in the nearby Con mine have $\delta^{18}O$ values near –14 per mil and have been interpreted to represent mixtures of ancient brines with more recent meteoric waters ($\delta^{18}O$ = –22‰; Frape et al., 1984; Frape and Fritz, 1987). Stage II fluids may represent the ancient (Proterozoic?) brine end member in this mixing. However, Bottomley et al. (1999) proposed a Devonian seawater source for the salinity in the modern brines, and thus, our fluid inclusion data may be unrelated to the deep mine waters.

Because of their high salinities (>25 wt % NaCl + $CaCl_2$), stage II brines were capable of remobilizing and transporting metals as chloride complexes (Seward and Barnes, 1997). English (1981) reported remobilization of gold from quartz veins in metasedimentary rocks east of the Giant mine by hydrothermal fluids of low temperature (~140°C) and moderate to high salinity (~11–30 wt % NaCl equiv). Similar $CaCl_2$-rich brines (100°–150°C) were responsible for base metal and gold remobilization from quartz veins in Proterozoic metasedimentary rocks of the mesothermal gold deposit at Curraghinalt, Northern Ireland (Wilkinson et al., 1999; Parnell et al., 2000).

Stage II veins in the Giant mine contain up to 5 vol percent base metal sulfides (principally galena), as well as up to 70 ppm silver and 8 ppm gold. The abundance of stage II veins in the Supercrest orebody (Fig. 2) at the northern end of the Giant mine may help explain locally enhanced gold ore grades. Observations by mine geologists also indicate that the ore grade improves as one approaches diabase dikes in the Supercrest portion of the mine (J. Todd, 1999, pers. commun.). Thus, stage II mineralization, while unrelated to original gold deposition at ~2.60 Ga, could be an important secondary process responsible for locally enriching metal grades at ~1.25 Ga.

### *Late vein and vug-filling stage III*

Stage III carbonates have a trend toward lower $\delta^{18}O$ and $\delta^{13}C$ values with decreasing age (Fig. 15a). The associated decrease in calculated $\delta^{18}O_{water}$ values from +1.1 to –6.8 per mil (Fig. 15b) indicates progressive introduction of less evolved, dilute (<6 wt % NaCl equiv) meteoric water into the Giant hydrothermal system at temperatures <115°C.

## Conclusions

By combining stable isotope and fluid inclusion techniques, it has been possible to see through the complexity of various

fluid overprints to deduce the chemistry of the early ore fluids and to suggest the mechanisms of gold ore deposition for the Giant orebodies. Refractory ores in the main alteration zone and gold-bearing quartz veins contained therein formed from chemically similar $CO_2$-$H_2O$-NaCl ore fluids whose oxygen isotope compositions are consistent with a metasedimentary source. These two styles of gold mineralization appear to be part of the same mineralizing event in which the style of mineralization was dictated by the mechanism of ore deposition. Refractory, sulfide-hosted gold mineralization resulted from reaction of mineralizing fluids with $Fe^{2+}$ in the metavolcanic wall rocks. Free-milling, gold-bearing quartz vein ores were deposited as a result of fluid unmixing, with loss of $H_2S$ to the vapor phase.

Gold-bearing quartz veins outside the main wall-rock alteration zone in the Giant mine were also deposited by unmixing of similar $H_2O$-$CO_2$-NaCl fluids. However, their fluids are isotopically distinct from those inside the alteration zone and need not be part of the sulfide-hosted gold-depositing event. They may instead represent a separate mineralizing event whose fluids and ore-forming constituents were derived solely from within metavolcanic rocks.

The distinction of multiple gold-forming events in the Giant mine is intriguing, because the overprint of one event upon the other may be a necessary condition for the development of world-class deposits in the Yellowknife district. As suggested by van Hees et al. (1999), the influences of both metavolcanic and metasedimentary ore fluid systems help explain how smaller greenstone belts, with limited volumes of metavolcanic rocks, can host substantial economic gold mineralization and has important implications for regional resource evaluation and exploration for gold deposits in greenstone belts.

## Acknowledgments

We acknowledge financial support from Royal Oak Mines Inc., EXTECH III, and the University of Missouri Research Board. We thank the Giant mine geology staff for their help in the field. Discussions with R. Hauser, T. Canam, J. Todd, and J. Armstrong were stimulating and productive. This paper is C.S. Lord Northern Geoscience Centre contribution 0002.

*September 20, 2002; July 6, 2004*

## REFERENCES

Anderson, A.T., Clayton, R.N., and Mayeda, T.K., 1971, Oxygen isotope thermometry of mafic igneous rocks: Journal of Geology, v. 79, p. 715–729.

Armstrong, J.P., 1997, Variations in silicate and sulfide mineral chemistry between free-milling "metallic" and refractory "invisible" gold ores, Con mine, Yellowknife, N.W.T.: Unpublished Ph.D. dissertation, London, ON, University of Western Ontario, 239 p.

——2002, Fault Lake, *in* Falck, H., ed., EXTECH III—the Yellowknife mining camp over 60 years of mining: Saskatoon, Saskatchewan, Geological Association of Canada, Fieldtrip Guide Book B-4, p. 103–105.

Atkinson, D.J., and van Breeman, O., 1990, Geology of the Western Plutonic Complex, southwestern Slave province: Late Archean crustal granites and gold mineralization in the Yellowknife district [abs.], *in* Goff, S.P., ed., Exploration and mining overview, 1990: Yellowknife, Northwest Territories, Indian and Northern Affairs Canada, p. 20.

Bakker, R.J., and Jansen, B.H., 1990, Preferential water leakage from fluid inclusions by means of mobile dislocation: Nature, v. 345, p. 58–60.

Bleeker, W., and Villeneuve, M., 1995, Structural studies along the Slave portion of the Snorcle transect: Calgary, Alberta, University of Calgary, Lithoprobe Report 44, p. 8–13.

Bleeker, W., Ketchum, J., Jackson, V.A., and Villeneuve, M.E., 1999, The Central Slave Basement Complex, Part I: Its structural topology and authochthonous cover: Canadian Journal of Earth Sciences, v. 36, p. 1083–1109.

Bodnar, R.J., and Vityk, M.O., 1994, Interpretation of microthermometric data for $H_2O$-NaCl fluid inclusions, *in* De Vino, B., and Frezzotti, M.L., eds., Fluid inclusions in minerals: Methods and applications: Blacksburg, Virginia Polytechnic Institute and State University, p. 117–130.

Bottomley, D.J., Katz, A., Chan, L.H., Starinsky, A., Douglas, M., Clark, I.D., and Raven, K.G., 1999, The origin and evolution of Canadian Shield brines: Evaporation or freezing of seawater? New lithium isotope and geochemical evidence from the Slave craton: Chemical Geology, v. 155, p. 295–320.

Boullier, A.-M., Firdaous, K., and Robert, F., 1998, On the significance of aqueous fluid inclusions in gold-bearing quartz vein deposits from the southeastern Abitibi subprovince (Quebec, Canada): Economic Geology, v. 93, p. 216–223.

Bowers, T.S., and Helgeson, H.C., 1983, Calculation of the thermodynamic and geochemical consequences of nonideal mixing in the system $H_2O$-$CO_2$-NaCl on phase relations in geologic systems: Metamorphic equilibria at high pressures and temperatures: American Mineralogist, v. 68, p. 1059–1075.

Boyle, R.W., 1954, A decrepitation study of quartz from the Campbell and Negus-Rycon shear zone systems, Yellowknife, Northwest Territories: Geological Survey of Canada Bulletin 30, 20 p.

——1961, The geology, geochemistry, and origin of the gold deposits of the Yellowknife district: Geological Survey of Canada Memoir 310, 191 p.

Brown, I.C., 1955, Late faults in the Yellowknife area: Geological Association of Canada, Toronto, Ontario, v. 7, Proceedings, p. 123–138.

Brown, N.N., 1992, Evolution of deformation and mineralization styles within the Giant shear zone complex, Yellowknife, Northwest Territories, Canada: Unpublished Ph.D. dissertation, University of California, Santa Barbara, 92 p.

Brown, C.E.G., and Dadson, A.S., 1953, Geology of the Giant Yellowknife mine: Canadian Institute of Mining and Metallurgy Transactions, v. 56, p. 59–76.

Brown, C.E.G., Dadson, A.S., and Wrigglesworth, L.A., 1959, On the ore-bearing structures of the Giant Yellowknife gold mine: Canadian Institute of Mining and Metallurgy Transactions, v. 62, p. 107–116.

Brown, P.E., and Hagemann, S.G., 1995, MacFlinCor and its application to fluids in Archean lode-gold deposits: Geochimica et Cosmochimica Acta, v. 19, p. 3943–3952.

Burrows, D.R., and Spooner, E.T.C., 1990, Geologic and fluid inclusion studies of an intrusion-hosted quartz-tourmaline-pyrite-gold vein system, Lamaque mine, Val d'Or, Quebec, *in* Robert, F., Sheahan, P.A., and Green, S.B., eds., Greenstone gold and crustal evolution, NUNA conference volume: St. Johns, NF, Geological Association of Canada, Mineral Deposits Division, p. 139–141.

Burruss, R.C., 1981a, Analysis of phase equilibria in C-O-H-S fluid inclusions: Mineralogical Association of Canada Short Course Handbook, v. 6, p. 39–73.

——1981b, Analysis of fluid inclusions: Phase equilibria at constant volume: American Journal of Science, v. 281, p. 1104–1126.

Campbell, N., 1947, The West Bay fault, Yellowknife: Transactions of the Canadian Institute of Mining and Metallurgy, v. 50, p. 509–526.

Chary, K.N., 1971, An isotopic and geochemical study of the gold-quartz veins in the Con-Rycon mine, Yellowknife: Unpublished M.Sc. thesis, Edmonton, University of Alberta, 90 p.

Clayton, R.N., and Mayeda, T.K., 1963, The use of bromine-pentafluoride in the extraction of oxygen from oxides and silicates for isotopic analyses: Geochimica et Cosmochimica Acta, v. 27, p. 43–52.

Clayton, R.N., O'Neil, J.R., and Mayeda, T.K., 1972, Oxygen isotope exchange between quartz and water: Journal of Geophysical Research, v. 77, p. 3057–3067.

Coleman, L.C., 1957, Mineralogy of the Giant Yellowknife gold mine, NWT: Economic Geology, v. 52, p. 400–425.

Costello, C.S., 1999, Geochemical and fluid inclusion studies of the Colomac mine, NWT, Canada: Unpublished M.S. thesis, University of Missouri, Columbia, 129 p.

Cousens, B.L., Gochnauer, K., Falck, H., van Hees, E.H., and Shelton, K.L., 1999, Pb-Pb isotopic dating of sulphide mineralization in the Yellowknife volcanic belt [abs.]: Yellowknife Geoscience Forum, 27th, Indian and Northern Affairs Canada, Yellowknife, Northwest Territories, Abstracts Volume, p. 12.

Craw, D., and Norris, R.J., 1993, Grain boundary migration of water and carbon dioxide during uplift of garnet-zone Alpine schist, New Zealand: Journal of Metamorphic Geology, v. 11, p. 371–378.

Crawford, M.L., 1981, Phase equilibria in aqueous fluid inclusions: Mineralogical Association of Canada Short Course Handbook, v. 6, p. 75–100.

Dadson, A.S., and Bateman, J.D., 1948, Giant Yellowknife mine: Canadian Institute of Mining and Metallurgy Jubilee Volume I, p. 273–283.

Danniel, A., Tödheide, K., and Franck, E.W., 1967, Verdampung, Gleichgewichte und kritische Kurven in den Systemen Attan/Wasser und n-Butan/Wasser bei Hohen Drucken: Chemisches Ingenieurwesen Technik, p. 816–822.

Davis, W.J., and Bleeker, W., 1999, Timing of plutonism, deformation and metamorphism in the Yellowknife domain, Slave province: Canadian Journal of Earth Sciences, v. 36, p. 1169–1187.

de Ronde, C.E.J., Spooner, E.T.C., de Wit, M.J., and Bray, C.J., 1992, Shear zone-related, Au quartz vein deposits in the Barberton greenstone belt, South Africa: Field and petrographic characteristics, fluid properties, and light stable isotope geochemistry: Economic Geology, v. 87, p. 366–402.

Diamond, L., 1992, Stability of $CO_2$ unmixing in the higher grade veins clathrate hydrate + $CO_2$ liquid + $CO_2$ vapor + aqueous KCl-NaCl solutions: Experimental determination and application to salinity estimates of fluid inclusions: Geochimica et Cosmochimica Acta, v. 56, p. 273–280.

Drury, S.A., 1977, Structures induced by granite diapirs in the Archean greenstone belt at Yellowknife, NWT: Implications for Archean geotectonics: Journal of Geology, v. 85, p. 345–358.

English, P.J., 1981, Gold-quartz veins in metasediments of the Yellowknife Supergroup, Northwest Territories: A fluid inclusion study: Unpublished M.Sc. thesis, Edmonton, University of Alberta, 108 p.

Falck, H., 1992, Gold mineralization in the Yellowknife mining district, NWT (NTS 85J/7,8,9,16): Geological Survey of Canada Open File 2484, p. 31–36.

Falck, H., Cousens, B., and Isachsen, C., 1999, Yet another new look at Yellowknife stratigraphy: Give me a break [abs.]: Yellowknife Geoscience Forum, 27th, Indian and Northern Affairs Canada, Yellowknife, Northwest Territories, Abstracts Volume, 16–18.

Fayek, M., and Kyser, T.K., 1995, Characteristics of auriferous and barren fluids associated with the Proterozoic Contact Lake gold deposit, Saskatchewan, Canada: Economic Geology, v. 90, p. 385–406.

Frape, S.K., and Fritz, P., 1987, Geochemical trends for groundwaters from the Canadian Shield: Geological Association of Canada Special Paper 33, p. 19–38.

Frape, S.K., Fritz, P., and McNutt, R.H., 1984, Water-rock interaction and chemistry of groundwaters from the Canadian Shield: Geochimica et Cosmochimica Acta, v. 48, p. 1617–1627.

Frith, R.A., 1993, Precambrian geology of the Indian Lake map area, District of Mackenzie, Northwest Territories: Geological Survey of Canada Memoir 424, 4 p.

Gehrig, M., 1980, Phasengleichgewichte und PVT-Daten ternärer Mischungen aus Wasser Kohlendioxid und Natriumchlorid bis 3 kbar und 550°C: Unpublished Ph.D. dissertation, Karlsruhe, Germany, Institut für Physikalische Chemie, Universität Karlsruhe, 109 p.

Goldfarb, R.J., Leach, D.L., and Pickthorn, W.J., 1988, Accretionary tectonics, fluid migration and gold genesis in the Pacific border ranges and coast mountains, southern Alaska, *in* Kisvarsanyi, G., and Grant, S. K., eds., North American conference on tectonic control of ore deposits and the vertical and horizontal extent of ore systems. Proceedings volume: Rolla, University of Missouri-Rolla Press, p. 67–79.

Grinenko, V.A., 1962, Preparation of sulfur dioxide for isotopic analysis: Zeitschrifte Neorganische Chemie, v. 7, p. 2478–2483.

Groves, D.I., and Phillips, N., 1987, The genesis and tectonic control on Archean gold deposits of the Western Australian shield—a metamorphic replacement model: Ore Geology Reviews, v. 2, p. 287–322.

Groves, D.I., Goldfarb, R.J., Gebre-Mariam, M., Hagemann, S.G. and Robert, F., 1998, Orogenic gold deposits: A proposed classification in the context of their crustal distribution and relationship to other gold types: Ore Geology Reviews, v. 13, p. 7–27.

Groves, D.I., Goldfarb, R.J., Robert, F., and Hart, C.J.R., 2003, Gold deposits in metamorphic belts: Overview of current understanding, outstanding problems, future research, and exploration significance: Economic Geology, v. 98, p. 1–29.

Helmstaedt, H., and Bailey, G., 1987, Problems of structural geology in the Yellowknife greenstone belt *in* Padgham, W.A., ed., Yellowknife guide book—a guide to the geology of the Yellowknife volcanic belt and its bordering rocks: St. Johns, Newfoundland, Geological Association of Canada, Mineral Deposits Division, p. 33–40.

Helmstaedt, H., and Padgham, W.A., 1986a, A new look at the stratigraphy of the Yellowknife Supergroup at Yellowknife, N.W.T.—implications for the age of gold-bearing shear zones and Archean basin evolution: Canadian Journal of Earth Sciences, v. 23, p. 454–475.

——1986b, Stratigraphy and structural setting of gold-bearing shear zones in the Yellowknife greenstone belt: Canadian Institute of Mining and Metallurgy Special Volume 38, p. 322–346.

Henderson, J.B., 1970, Stratigraphy of the Yellowknife Supergroup, Yellowknife Bay-Prosperous Lake area, District of MacKenzie: Geological Survey of Canada Paper 70-26, 12 p.

——1972, Sedimentology of Archean turbidites at Yellowknife, Northwest Territories: Canadian Journal of Earth Sciences, v. 9, p. 882–902.

——1975, Sedimentology of the Archean Yellowknife Supergroup at Yellowknife, District of MacKenzie: Geological Survey of Canada Bulletin 246, 62 p.

——1985, Geology of the Yellowknife-Hearne Lake area, District of MacKenzie: A segment across an Archean basin: Geological Survey of Canada Memoir 414, 135 p.

Henderson, J.F., and Brown, I.C., 1966, Geology and structure of the Yellowknife greenstone belt, District of MacKenzie: Geological Survey of Canada Bulletin 141, 87 p.

Hodgson, C.H., Love, D.A., and Hamilton, J.V., 1993, Giant mesothermal gold deposits: Descriptive characteristics, genetic model, and exploration area selection criteria: Society of Economic Geologists Special Publication 2, p. 157–211.

Ho, S.E., Groves, D.I., McNaughton, N.J., and Mikucki, E.J., 1992, The source of ore fluids and solutes in Archean lode-gold deposits of Western Australia: Journal of Volcanology and Geothermal Research, v. 50, p. 173–196.

Hollister, L.S., 1990, Enrichment of $CO_2$ in fluid inclusions in quartz by removal of $H_2O$ during crystal-plastic deformation: Journal of Structural Geology, v. 12, p. 895–901.

Isachsen, C.E., 1992, U-Pb zircon geochronology of the Yellowknife volcanic belt and subjacent rocks, N.W.T., Canada: Constraints on the timing, duration, and mechanics of greenstone belt formation: Unpublished Ph.D. dissertation, St. Louis, MO, Washington University, 164 p.

Isachsen, C.E., and Bowring, S.A., 1994, Evolution of the Slave craton: Geology, v. 22, p. 917–920.

——1997, The Bell Lake Group and Anton Complex: A basement-cover sequence beneath the Yellowknife greenstone belt revealed and implicated in greenstone belt formation: Canadian Journal of Earth Sciences, v. 34, p. 169–178.

Jia, Y., Kerrich, R., and Goldfarb, R., 2003, Metamorphic origin of ore-forming fluids for orogenic gold-bearing quartz vein systems in the North American Cordillera: Constraints from a reconnaissance study of $\delta^{15}N$, $\delta D$, and $\delta^{18}O$: Economic Geology, v. 98, p. 109–123.

Johnson, E.L., and Hollister, L.S., 1995, Syndeformational fluid trapping in quartz: Determining the pressure-temperature conditions of deformation from fluid inclusions and the formation of pure $CO_2$ fluid inclusions during grain boundary migration: Journal of Metamorphic Geology, v. 13, p. 239–249.

Kerrich, R., 1981, Archean lode gold deposits: A synthesis of data on metal distribution, fluid inclusions and stable isotopes, with special reference to Yellowknife, *in* Morton, R.D., ed., Proceedings of the gold workshop, Yellowknife Geo-Workshop Committee: Yellowknife, Northwest Territories, Indian and Northern Affairs Canada, p. 95–173.

——1987, The stable isotope geochemistry of Au-Ag vein deposits in metamorphic rocks: Mineralogical Association of Canada Short Course Handbook, v. 13, p. 287–336.

——1989, Geodynamic setting and hydraulic regimes: Shear zone hosted mesothermal gold deposits: Geological Association of Canada Short Course Notes 6, p. 89–128.

Kerrich, R., and Allison, I., 1978, Vein geometry and hydrostatics during Yellowknife mineralization: Canadian Journal of Earth Sciences, v. 15, p. 1653–1660.

Kerrich, R., and Fyfe, W.S., 1981, The gold-carbonate association: Source of $CO_2$ and $CO_2$-fixation reactions in Archean lode gold deposits: Chemical Geology, v. 33, p. 265–294.

——1987, The formation of gold deposits with particular reference to Archean greenstone belts and Yellowknife: A synthesis of geochemical data, *in* Padgham, W.A., ed., Yellowknife guide book—a guide to the geology of

the Yellowknife volcanic belt and its bordering rocks: St. Johns, Newfoundland, Geological Association of Canada, Mineral Deposits Division, p. 155–174.

——1988, The formation of gold deposits with particular reference to Archean greenstone belts and Yellowknife: Yellowknife, Northwest Territories, Indian and Northern Affairs Canada, Contributions to the Geology of the Northwest Territories, v. 3, p. 63–95.

Kerrich, R., and Kamineni, D.C., 1988, Characteristics and chronology of fracture-fluid infiltration in the Archean, Eye Dashwa Lakes pluton, Superior province: Evidence from H, C, O-isotopes and fluid inclusions: Contributions to Mineralogy and Petrology, v. 99, p. 430–445.

Kerrich, R., and King, R., 1993, Hydrothermal zircon and baddaeleyite in Val-d'Or Archean mesothermal gold deposits: Characteristrics, compositions, and fluid inclusion properties, with implications for timing of primary gold mineralization: Canadian Journal of Earth Sciences, v. 30, p. 2334–2351.

Kerrick, D.M., and Jacobs, G.K., 1981, A modified Redlich-Kwong equation for $H_2O$, $CO_2$ and $H_2O$-$CO_2$ mixtures at elevated pressures and temperatures: American Journal of Science, v. 281, p. 735–767.

Kerswill, J.A., and Falck, H., 2002, Regional metallogeny of the Yellowknife EXTECH area, Northwest Territories, Canada [abs.]: Geological Association of Canada-Mineralogical Association of Canada annual meeting, Saskatoon, Canada, May 27–29, 2002, Program and Abstracts, v. 27, p. 59–60.

Kerswill, J., Falck, H., and Cousens, B., 2002, Metallogeny of the Yellowknife area: Saskatoon, Saskatchewan, Geological Association of Canada, Fieldtrip Guide Book B-4, p. 44–55.

Kesler, S.E., 1991, Nature and composition of mineralizing solutions: NUNA Conference on Greenstone Gold and Crustal Evolution, Val d'Or, Quebec, May 24–27, 1990, Proceedings, p. 86–90.

Ketchum, J., and Bleeker, W., 2000, New field and U-Pb data from the Central Slave Cover Group near Yellowknife and the Central Slave Basement Complex at Point Lake, Slave-Northern Cordillera lithospheric evolution transect: Calgary, AB, University of Calgary, Lithoprobe Report 72, p. 27–31.

Klemd, R., 1998, Comment on the paper by Schmidt Mumm et al.: High $CO_2$ content of fluid inclusions in gold mineralizations in the Ashanti belt, Ghana: A new category of ore-forming fluids?: Mineralium Deposita, v. 33, p. 317–319.

Klemd, R., Hirdes, W., Olesch, M., and Oberthür, T., 1993, Fluid inclusions in quartz-pebbles of the gold-bearing Tarkwaian conglomerates of Ghana as guides to their provenance area: Mineralium Deposita, v. 28, p. 334–343.

Klemd, R., Oberthür, T., and Ouedrago, A., 1997, Gold-telluride mineralization in the Birimian at Diabatou, Burkina Faso: Journal of African Earth Science, v. 24, p. 227–239.

Kyser, T.K., O'Neil, J.R., and Carmichael, I.S.E., 1981, Oxygen isotope thermometry of basic lavas and mantle nodules: Contributions to Mineralogy and Petrology, v. 77, p. 11–23.

——1982, Genetic relations among basic lavas and ultramafic nodules: Evidence from oxygen isotope compositions: Contributions to Mineralogy and Petrology, v. 81, p. 88–102.

Lamb, W.M., 1993, Retrograde deformation within the Carthage-Colton zone as recorded by fluid inclusions and feldspar compositions: Tectonic implications for the southern Grenville province: Contributions to Mineralogy and Petrology, v. 114, p. 379–394.

LeCheminant, A.N., and Heaman, L.M., 1989, MacKenzie igneous events, Canada: Middle Proterozoic hotspot magmatism associated with ocean opening: Earth and Planetary Science Letters, v. 96, p. 38–48.

Lord, C.S., 1951, Mineral industry of the District of MacKenzie, Northwest Territories: Geological Survey of Canada Memoir 261, 325 p.

MacLachlan, K., and Davis, W.J., 2002, Uranium-lead ages of Defeat granitoid rocks near the Con mine, Northwest Territories: Geological Survey of Canada Current Research 2002-F1, 9 p.

Manu, J., 1993, Gold deposits of Birimian greenstone belt in Ghana: Hydrothermal alteration and thermodynamics: Braunschweiger Geol-Paläontol., Dissertationen, v. 17, 166 p.

Matsuhisa, Y., Goldsmith, J.R., and Clayton, R.N., 19729, Oxygen isotope fractionation in the system quartz-albite-anorthite-water: Geochimica et Cosmochimica Acta, v. 43, p. 1131–1140.

McCrea, J.M., 1950, The isotope geochemistry of carbonates and a paleotemperature scale: Journal of Chemistry and Physics, v. 18, p. 849–857.

McMenamy, T.A., 1999, Geochemical studies of greenstone-hosted gold deposits of the Giant mine, NWT, Canada: Unpublished M.S. thesis, University of Missouri, Columbia, 95 p.

Nesbitt, B.E., Murowchick, J.B., and Muehlenbachs, K., 1986, Dual origins of lode gold deposits in the Canadian Cordillera: Geology, v. 14, p. 506–509.

O'Neil, J.R., and Taylor, H.P., Jr., 1967, The isotope and cation exchange chemistry of feldspars: American Mineralogist, v. 52, p. 1414–1437.

O'Neil, J.R., Clayton, R.N., and Mayeda, T.K., 1969, Oxygen isotope fractionation in divalent metal carbonates: Journal of Chemistry and Physics, v. 51, p. 5547–5558.

Ootes, L., Lentz, D.R., Falck, H., Creaser, R.A., and Ketchum, J., 2002, U-Pb zircon and Re-Os molybdenite ages from the Ryan Lake pluton and Duckfish aplite: Results, implications, and potential of the Re-Os chronometer in the Yellowknife greenstone belt: Yellowknife Geoscience Forum, 30th, Indian and Northern Affairs Canada, Yellowknife, Northwest Territories, Abstracts Volume, p. 49–50.

Parnell, J., Earls, G., Wilkinson, J.J., Hutton, D.H.W., Boyce, A.J., Fallick, A.E., Ellam, R.M., Gleeson, S.A., Moles, N.R., Carey, P.F., and Legg, I., 2000, Regional fluid flow and gold mineralization in the Dalradian of the Sperrin Mountains, Northern Ireland: Economic Geology, v. 95, p. 1389–1416.

Pickthorn, W.J., Goldfarb, R.J., and Leach, D.L., 1987a, "Mesothermal" gold—a metamorphic connection?: U. S. Geological Survey Circular 995, 57 p.

———1987b, Comment and reply on "Dual origins of lode gold deposits in the Canadian Cordillera:" Geology, v. 15, p. 471–472.

Ramboz, C., Pichavant, M., and Weisbrod, A., 1982, Fluid immiscibility in natural processes: Use and misuse of fluid inclusion data, II. Interpretation of fluid inclusion data in terms of immiscibility: Chemical Geology, v. 37, p. 29–48.

Relf, C., 1988, The alteration history of a series of shear zones, Mirage Islands, Yellowknife Bay, N.W.T.: Unpublished M.Sc. thesis, St. Johns, Memorial University of Newfoundland, 125 p.

Robert, F., 1990, An overview of gold deposits in the eastern Abitibi belt: Canadian Institute of Mining and Metallurgy Special Volume 43, p. 93–105.

Robert, F., and Kelly, W.C., 1987, Ore-forming fluids in Archean gold-bearing quartz veins at the Sigma mine, Abitibi greenstone belt, Quebec, Canada: Economic Geology, v. 82, p. 1464–1482.

Robert, F., and Poulsen, K. H., 1997, World-class Archean gold deposits in Canada: An overview: Australian Journal of Earth Sciences, v. 44, p. 329–351.

Roedder, E., 1984, Fluid inclusions: Reviews in Mineralogy, v. 12, 644 p.

Roedder, E., and Bodnar, R.J., 1980, Geologic pressure determinations from fluid inclusion studies: Annual Reviews in Earth and Planetary Sciences, v. 8, p. 263–301.

Sakai, H., 1968, Isotopic properties of sulfur compounds in hydrothermal processes: Geochemistry Journal, v. 12, p. 29–49.

Samson, I.M., Bulent, B., and Holm, P.E., 1997, Hydrothermal evolution of auriferous shear zones, Wawa, Ontario: Economic Geology, v. 92, p. 325–342.

Schmidt Mumm, A., Oberthür, T., Vetter, U., and Blenkinsop, T.G., 1997, High $CO_2$ content of fluid inclusions in gold mineralizations on the Ashanti belt, Ghana: A new category of ore forming fluids?: Mineralium Deposita, v. 32, p. 107–118.

Seward, T.M., and Barnes, H.L., 1997, Metal transport by hydrothermal ore fluids, *in* Barnes, H.L., ed., Geochemistry of hydrothermal ore deposits, 3rd ed.: New York, Wiley and Sons, p. 435–486.

Shelton, K.L., and Orville, P.M., 1980, Formation of synthetic fluid inclusions in natural quartz: American Mineralogist, v. 65, p. 1233–1236.

Shelton, K.L., So, C.S., and Chang, J.S., 1988, Gold-rich mesothermal vein deposits of the Republic of Korea: Geochemical studies of the Jungwon gold area: Economic Geology, v. 83, p. 1221–1237.

Shelton, K.L., Costello, C.S., and van Hees, E.H., 2000, Contrasting styles of Archean greenstone gold deposition: Colomac gold mine, Canadian Northwest Territories: Journal of Geochemical Exploration, v. 69–70, p. 303–307.

Siddorn, J.P., and Cruden, A.R., 2000, Timing of gold mineralisation in the Giant and Con deposits, Yellowknife, Canada [abs.]: Yellowknife Geoscience Forum, 28th, Indian and Northern Affairs Canada, Yellowknife, Northwest Territories, Abstracts Volume, p. 63–64.

Siddorn, J.P., Cruden, A.R., Armstrong, J.P., Hauser, R.L., and Kirkham, G., 2005, The Giant-Con gold deposits: Integrated structural and mineralisation history, *in* Falck, H., Anglin, L., and Wright, D., eds., EXTECH III Yellowknife gold: A multidisciplinary examination of gold mineralization in the Yellowknife greenstone belt, Northwest Territories: Geological Association of Canada, Mineral Deposits Division, Special Publication (in press).

So, C.S., Seong-Taek, Y., and Shelton, K.L., 1995, Mesothermal gold vein mineralization of the Samdong mine, Youngdong mining district, Republic of Korea: Mineralium Deposita, v. 30, p. 384–396.

Steffanski, M.J., and Halverson, G.B., 1992, Gold recovery improvement investigations at Giant Yellowknife mine: Geological Survey of Canada Open File 2484, p. 217–219.

Taylor, H.P., Jr., 1968, The oxygen isotope geochemistry of igneous rocks: Contributions to Mineralogy and Petrology, v. 19, p. 1–17.

Thiery, R., van den Kerkhof, A.M., and Dubessy, J., 1994, vX properties modelling of $CH_4$-$CO_2$ and $CO_2$-$N_2$ fluid inclusions (T <31°C, P <400 bars): European Journal of Mineralogy, v. 6, p. 753–771.

Thompson, P.H., 2002, Metamorphism of the Yellowknife greenstone belt: Saskatoon, Saskatchewan, Geological Association of Canada Fieldtrip Guide Book B-4, p. 32–43.

van Hees, E.H.P., and Shelton, K.L., 2002a, Miramar Con mine—wall rock alteration: Saskatoon, Saskatchewan, Geological Association of Canada Fieldtrip Guide Book B-4, p. 91–93.

——2002b, Giant mine—Cameron zone: Saskatoon, Saskatchewan, Geological Association of Canada Fieldtrip Guide Book B-4, p. 97–102.

van Hees, E.H.P., Shelton, K.L., McMenamy, T.A., Ross, L.M., Jr., Cousens, B.L., Falck, M., Robb, M.E., and Canam, T.W., 1999, Metasedimentary influence on metavolcanic-rock-hosted greenstone gold deposits: Geochemistry of the Giant mine, Yellowknife, Northwest Territories, Canada: Geology, v. 27, p. 71–74.

van Hees, E.H.P., Kirkham, G.D., Sirbescu, M.-L., Shelton, K.L., Hauser, R., and Falck, H., 2005, Lithogeochemical halos around Yellowknife gold deposits: Nature of large alteration halos and their implications, *in* Falck, H., Anglin, L., and Wright, D., eds., EXTECH III Yellowknife gold: A multidisciplinary examination of gold mineralization in the Yellowknife greenstone belt, Northwest Territories: Geological Association of Canada, Mineral Deposits Division, Special Publication, in press.

Walsh, J.F., Kesler, S.E., Duff, D., and Cloke, P. L., 1988, Fluid inclusion geochemistry of high-grade, vein-hosted gold ore at the Pamour mine, Porcupine Camp, Ontario: Economic Geology, v. 83, p. 1347–1367.

Wanless, R.K., Boyle, R.W., and Lowdon, J.A., 1960, Sulfur isotope investigation of the gold-quartz deposits of the Yellowknife district: Economic Geology, v. 55, p. 1591–1619.

Watson, E.B., and Brennan, J.M., 1987, Fluids in the lithosphere. 1. Experimentally-determined wetting characteristics of $CO_2$-$H_2O$ fluids and their implications for fluid transport, host-rock physical properties, and fluid inclusion formation: Earth and Planetary Science Letters, v. 85, p. 497–515.

Webb, D.R., 1992, The geochemistry and structural controls of auriferous shear zones at Yellowknife, Mackenzie district, Northwest Territories, Canada: Unpublished Ph.D. dissertation, London, ON, University of Western Ontario, 136 p.

Wilkinson, J.J., Boyce, A., Earls, G., and Fallick, A.E., 1999, Gold mineralization by low-temperature brines: Evidence from the Curraghinalt gold deposit, Northern Ireland: Economic Geology, v. 94, p. 289–296.

Woodall, R., 1988, Gold in 1988: Geological Society of Australia Abstracts Series 22, p. 1–12.

Zhang, Y.G., and Frantz, J.D., 1989, Experimental determination of the compositional limits of immiscibility in the system $CaCl_2$-$H_2O$-$CO_2$ at high temperatures and pressures using synthetic fluid inclusions: Chemical Geology, v. 74, p. 289–308.